Sparse Decentralized Federated Learning

Shan Sha, Shenglong Zhou, Lingchen Kong, Geoffrey Ye Li, Fellow, IEEE

Abstract—Decentralized Federated Learning (DFL) enables collaborative model training without a central server but faces challenges in efficiency, stability, and trustworthiness due to communication and computational limitations among distributed nodes. To address these critical issues, we introduce a sparsity constraint on the shared model, leading to Sparse DFL (SDFL), and propose a novel algorithm, CEPS. The sparsity constraint facilitates the use of one-bit compressive sensing to transmit one-bit information between partially selected neighbour nodes at specific steps, thereby significantly improving communication efficiency. Moreover, we integrate differential privacy into the algorithm to ensure privacy preservation and bolster the trustworthiness of the learning process. Furthermore, CEPS is underpinned by theoretical guarantees regarding both convergence and privacy. Numerical experiments validate the effectiveness of the proposed algorithm in improving communication and computation efficiency while maintaining a high level of trustworthiness.

Index Terms—SDFL, one-bit compressive sensing, communication and computational efficiency, differential privacy

I. INTRODUCTION

PEDERATED learning (FL [1], [2]) is a machine learning framework that enables called across multiple nodes (e.g., devices or entities) by exchanging local parameters instead of raw data. This approach has gained widespread attention with the fast development of Internet of Things, where data are stored in distributed devices and it is impossible to collect raw data as in traditional machine learning settings due to the restriction of communication resource, data privacy concern, or law regulations. In the most predominate FL setting, a central server or coordinator is required to aggregate parameters from all nodes, update a global model, and broadcast it back to the nodes for further training, which is referred to as centralized federated learning (CFL). In contrast, decentralized federated learning (DFL [3], [4]), as a new setting of FL, eliminates the need for a central server, allowing nodes to communicate directly with their neighbours based on a predefined network topology and perform local update. DFL addresses the communication bottleneck inherent in CFL by distributing information exchange among all nodes, which avoids the limitation of singlepoint failure and improves fault tolerance. Moreover, DFL can enhance the robustness of the learning process because nodes constantly update their knowledge within the communication

This work was supported by the Fundamental Research Funds for the Central Universities and the Talent Fund of Beijing Jiaotong University. Corresponding author: Shenglong Zhou.

Shan Sha, Lingchen Kong, and Shenglong Zhou are with the School of Mathematics and Statistics, Beijing Jiaotong University, Beijing, China. E-mail: {20118023, lchkong, shlzhou}@bjtu.edu.cn. Geoffrey Ye Li are with the Department of Electrical and Electronic Engineering, Faculty of Engineering, Imperial College London, London, U.K. E-mail: geoffrey.li@imperial.ac.uk.

network and can achieve comparable or even superior accuracy and computational efficiency compared to CFL [5].

Despite these advantages, the decentralized setting of DFL also introduces new challenges. Communication efficiency remains a primary concern, involving the selection of neighbour nodes for communication and the transmission of information without a central server. The absence of the central aggregator complicates theoretical analysis, as it requires managing multiple local models at each step instead of a single global model. Trustworthiness is another critical issue, although FL inherently prevents raw data sharing, it has been shown in [6] that local model parameters can still leak private information. Therefore, implementing privacy-preserving techniques is essential in FL, and even more so in DFL, where decentralized communication is more susceptible to attacks compared to communication with a protected central server.

A. Prior Arts

We begin by reviewing foundational DFL algorithms and then discuss important DFL topics such as communication efficiency, communication topology, and privacy preservation.

- 1) Foundational DFL Algorithms: A decentralized parallel stochastic gradient descent (D-PSGD) method has been introduced by [5] to address DFL by performing SGD scheme synchronously and parallelly across all nodes, with the communication protocol defined by a symmetric doubly stochastic matrix. Subsequently, various methods based on this decentralized SGD scheme have been proposed. [12] presented a Bayesian-like approach by introducing of a belief over the model parameter space on local nodes, enabling nodes to communicate with fewer neighbours. [13] offered a decentralized framework based on the Interplanetary File System to overcome limitations of CFL, such as single points of failure and bandwidth bottlenecks. [14] developed a robust solution for DFL in unreliable communication environments by updating model parameters with partially received messages and optimizing mixing weights. To address the overfitting issue inherent in DFL, [9] incorporated Sharpness-Aware Minimization to improve generalization performance and considers multiple inter-node communications to enhance model consistency. Other related research includes [15, 16].
- 2) Communication Efficiency: Communication efficiency is a primary goal in federated learning research, whether in centralized or decentralized settings. Two main strategies to reduce communication costs are data compression and reducing the number of communication rounds. In [8], a decentralized version of the federated averaging algorithm with momentum (DFedAvgM) has been proposed. It performed multiple local updates with momentum and included one communication step per round to enhance efficiency. A quantized version

	Ref.	Local Updates	Device Participation	Communication Topology	Information Compression	Privacy Protection
D-PSGD	[5]	Single	Full	Mixing Matrix	None	None
DCD-PSGD	[7]	Single	Full	Mixing Matrix	Difference Compression	None
D-FedAvgM	[8]	Multiple	Full	Mixing Matrix	Quantization	None
DFedSAM	[<mark>9</mark>]	Single	Full	Mixing Matrix	None	None
MATCHA	[10]	Multiple	Partial	Dynamic Network	None	None
DP-DSGT	[11]	Single	Full	Mixing Matrix	None	Differential Privacy
CFPS	Our	Multiple	Partial	Dynamic Network	1RCS	Differential Privacy

TABLE I: Comparisons of Different Algorithms.

of DFedAvgM was also investigated to reduce communication overhead further. [17] proposed a general framework of DFL to achieve a better balance between communication efficiency and model consensus with a similar strategy. Several works have explored different compression strategies in DFL. In [7], two variants based on D-PSGD were proposed to enhance communication efficiency using extrapolation compression and difference compression strategies. [18] and [19] provided a general quantized communication framework for DFL with arbitrary compression operators. [20] also discussed communication-efficient methods in DFL.

- 3) Communication Topology: Communication topology significantly affects the convergence speed and efficiency of DFL, as it determines which neighbours each node communicates within each round. Optimizing the communication topology can lead to faster convergence and reduced communication overhead. MATCHA [10] speeded up decentralized SGD by prioritizing critical communication links and allowing parallel communication over disjoint links to minimize communication delays while maintaining fast convergence rates. GossipFL [21] proposed a sparsification model to reduce communication traffic and introduced an adaptive peer-selection mechanism to improve bandwidth utilization while preserving model convergence. Other works such as [22, 23] also addressed the impact of communication topology on DFL performance.
- 4) Privacy Preservation: Privacy preservation is a key feature of FL, ensuring that raw data is not shared with a central server or other nodes. However, if transmitted information (e.g., gradients) is intercepted by adversaries, the raw data can be reconstructed, leading to privacy breaches [24, 25]. The importance of privacy preservation, along with other trustworthy artificial intelligence (AI) components such as fairness and robustness, is increasingly recognized in the development of secure and reliable AI systems ([26-28]). Existing work in FL mainly focuses on deploying privacypreserving techniques like differential privacy (DP) in centralized FL [29-32]. In the context of DFL, research on privacy preservation is relatively limited. [33] proposed a differential privacy decentralized optimization algorithm based on SGD, providing privacy guarantees without relying on a central server. [34] considered static and dynamic consensusbased gradient methods where DP is combined with gossip algorithms to ensure privacy. [11] provided a generalization of D-PSGD with privacy guarantee.

B. Our contribution

The main contribution of this paper is the development of a novel SDFL algorithm, CEPS (standing for a Communication-

Efficient and Private method for SDFL), designed to address multiple critical challenges in DFL. Table I compares CEPS with six DFL algorithms, highlighting its ability to deal with a wider range of challenges simultaneously. This capability stems from several key advantages outlined below.

- Communication efficiency. Due to the integration of a sparsity constraint in the learning model, we harness the 1BCS technique to exchange one-bit signals when two neighbour nodes communicate with each other. Consequently, the transmitted content is significantly lessened. To the best of our knowledge, we have not come across similar efforts to incorporate 1BCS into DFL. Simultaneously, each node communicates with its neighbours only at specific steps rather than every step to update its parameters, thereby greatly reducing the number of communication rounds.
- Computational efficiency. It results from two factors. Every node solves subproblems without much computational endeavour using closed-form solutions. Complex elements, such as gradients, are computed at designated steps and remain unchanged during other steps.
- Robustness against stragglers. Each node can selectively
 pick partial neighbour nodes to collect messages to update
 its parameter, so neighbours who suffer from unreliable and
 imperfect communication links can be paid less attention.
- Privacy Protection. By incorporating the Gaussian mechanism, we provide a rigorous privacy guarantee for data across all nodes under a certain noise perturbation level.
- Theoretical Guarantee. We provide a convergence bound of CEPS under common assumptions in DFL analysis, which ensures the algorithm gives an approximation solution in terms of the average global gradient.
- Desirable numerical performance. Numerical experiments
 have demonstrated that the 1BCS technique enables effective communication and thus allows the proposed algorithm
 to achieve desirable training accuracy. We also compare
 CEPS with several leading DFL algorithms, highlighting its
 great potential in dealing with the challenges of imperfect
 and unreliable communication environments.

We point out that part of our work has been previously published in [35]. In this paper, we extend the original study with three major contributions: First, we enhance the algorithm by incorporating DP to ensure privacy protection. Second, we provide rigorous convergence proofs, offering strong theoretical guarantees. Third, extensive numerical experiments and comparisons with other DFL algorithms validate the effectiveness and performance of our approach. These improvements significantly advance the initial ideas and demonstrate the enhanced capabilities of CEPS.

C. Organization

The paper is organized as follows. Section II presents all notation, the models of interest, and the definition of DP. In Section III, we develop the algorithm and highlight its several advantageous properties. In section IV, we provide theoretical analysis including the convergence and privacy guarantee. In Section V, we conduct some numerical experiments to demonstrate the performance of the proposed algorithm. Concluding remarks are given in the last section.

II. PRELIMINARIES

In this section, we introduce the notation used in this paper, the problems of DFL and SDFL, and the definition of DP.

A. Notation

We use plain, bold, and capital letters to present scalars, vectors, and matrices, respectively, e.g., n and σ are scalars, \mathbf{w} and $\boldsymbol{\xi}$ are vectors, \mathbf{W} and $\boldsymbol{\Xi}$ are matrices. Let \mathbb{R}^n denote the n-dimensional Euclidean space equipped with inner product $\langle \cdot, \cdot \rangle$, defined by $\langle \mathbf{w}, \mathbf{v} \rangle := \sum_{i=1}^m w_i v_i$, where ':=' means 'define'. We use $\|\cdot\|$ to denote the Euclidean norm for vectors and the Frobenius norm for matrices, namely, $\|\mathbf{w}\| = \sqrt{\sum_i w_i^2}$ and $\|\mathbf{W}\| = \sqrt{\sum_{ij} W_{ij}^2}$. The sign function is defined as $\operatorname{sign}(t) = 1$ if t > 0 and -1 otherwise and is applied element-wisely for vectors: $\operatorname{sign}(\mathbf{w}) = (\operatorname{sign}(w_1), \operatorname{sign}(w_2), \dots, \operatorname{sign}(w_n))^{\top}$, where $^{\top}$ represents the transpose. The projection of a point \mathbf{w} onto Ω is defined by

$$\mathbb{P}_{\Omega}(\mathbf{w}) \in \operatorname{argmin}_{\mathbf{z} \in \Omega} \|\mathbf{z} - \mathbf{w}\|^2,$$

which keeps the first s largest (in absolute value) entries in Ω and sets the remaining entries to be zero. Finally, by letting $\mathbf{W} := (\mathbf{w}_1, \mathbf{w}_2, \cdots, \mathbf{w}_m)$, the sparse projection operator on matrix \mathbf{W} is defined as

$$\mathbb{P}_{\Omega}(\mathbf{W}) = (\mathbb{P}_{\Omega}(\mathbf{w}_1), \mathbb{P}_{\Omega}(\mathbf{w}_2), \cdots, \mathbb{P}_{\Omega}(\mathbf{w}_m)).$$

B. Decentralized Federated Learning

Given m nodes $V:=\{1,2,\cdots,m\}$, each node i has a loss function $f_i(\cdot):=f_i\left(\cdot;D_i\right)$ associated with private dataset D_i , where $f_i:\mathbb{R}^n\to\mathbb{R}$ is continuous and bounded from below. In a DFL scenario, a general setting of communication topology can be given as follows: Each node i only exchanges messages with its neighbours $j\in N_i$, where $N_i\subseteq V$ consists of node i and the nodes connected to node i. Overall, we obtain a graph G=(V,E), where $E=\{(i,j):j\in N_i,i\in V\}$ is the set of edges. Based on this setting, the target graph is undirected, namely if $i\in N_j$ then $j\in N_i$. Hereafter, we always assume graph G is connected. The task of DFL is to train a model by solving the following optimization problem

$$f^* := \min_{\mathbf{w}_i \in \mathbb{R}^n} \sum_{i \in V} f_i(\mathbf{w}_i),$$
s.t. $\mathbf{w}_i = \mathbf{w}_j, \ (i, j) \in E,$ (DFL)

where $\mathbf{w}_i, i \in V$ are the parameters to be learned. Since graph G is connected, it follows $\mathbf{w}_1 = \mathbf{w}_2 = \cdots = \mathbf{w}_m$. As each f_i is bounded from below, we have $f^* > -\infty$. Under the setting of DFL, each node trains its own local model \mathbf{w}_i , and the model consensus is realized by communication among nodes.

C. Sparse DFL

The objective of our work is to train a model by solving the following sparsity constrained DFL model,

$$\min_{\mathbf{W}} \sum_{i \in V} f_i(\mathbf{w}_i)
\text{s.t.} \quad \mathbf{w}_i = \mathbf{w}_i, \ (i, j) \in E, \quad \mathbf{w}_i \in \Omega, \ i \in V,$$

where $\mathbf{W} := (\mathbf{w}_1, \mathbf{w}_2, \cdots, \mathbf{w}_m) \in \mathbb{R}^{n \times m}$ and Ω is a sparsity constraint defined by

$$\Omega := \{ \mathbf{w} \in \mathbb{R}^n : \|\mathbf{w}\|_0 \le s \}.$$

Here, $\|\mathbf{w}\|_0$ is known as a zero norm that counts the number of non-zero entries of \mathbf{w} and $s \ll n$ is a given sparsity level. The motivation for studying (SDFL) arises from two aspects. First, the incorporation of a sparsity constraint drastically reduces the volume of transmitted messages, thereby significantly enhancing communication efficiency, as demonstrated in Section III-C and supported by our numerical experiments (see Fig. 6). Second, model (SDFL) is a special case of sparse optimization, rooted in the principles of compressive sensing [36, 37]. As stated in [38–40], leveraging sparsity provides computationally feasible ways to reveal the structure of massive high-dimensional data, giving rise to a large repertoire of efficient algorithms for fast computation. Overall, (SDFL) ensures both high communication efficiency and computational feasibility.

D. Differential Privacy

DP is intrinsically a property of a randomized mechanism [41]. We adopt the definition of DP from [42].

Definition 1. (Differential Privacy) A randomized mechanism: $\mathcal{M}: D \to \mathbb{R}$ is (ϵ, δ) -differentially private if, for any two adjacent datasets $H, H' \subseteq D$ and any $S \subseteq \mathbb{R}$ satisfies

$$\Pr[\mathcal{M}(H) \in S] \le e^{\varepsilon} \Pr[\mathcal{M}(H') \in S] + \delta,$$
 (1)

where adjacent datasets refer to H and H' are at the same size and differ in exactly one record.

From the perspective of algorithmic design, an algorithm is of DP if it generates a randomized response that satisfies condition (1). This ensures that the outputs are statistically similar for adjacent datasets, thereby preventing adversaries from inferring specific information about individual data points. The DP of an algorithm is typically achieved by adding noise drawn from a specific probability distribution. The magnitude of this noise depends on the functional sensitivity, which quantifies how much the output can change in response to variations in the input.

Definition 2. (Function Sensitivity) The global sensitivity of an algorithm (function) $A: D \to \mathbb{R}$ is the maximum output difference for any two adjacent datasets H and H',

$$\eta(\mathcal{A}) = \max_{H, H' \subset D} \|\mathcal{A}(H) - \mathcal{A}(H')\|_2. \tag{2}$$

It is obvious from (1) and (2) that smaller values of ε and δ provide stronger privacy protection, while a larger $\eta(A)$ indicates higher sensitivity to input changes, necessitating more

Algorithm 1: CEPS: Communication-Efficient and Private method for SDFL.

Initialize $\mathbf{W}^0 = 0$ and $\mu > 0$. for every node $i \in V = \{1, 2, \cdots, m\}$ do

Initialize an integer $\kappa_i > 0$, three real numbers $\varrho_i > 0, \gamma_i > 0, \sigma_i > 0$, and an encoding matrix $\Phi_i \in \mathbb{R}^{d_i \times n}$.

Initialize $m_i^{-1} = |N_i|$ and $\mathbf{u}_i^{-1} = -\nabla f_i(\mathbf{w}_i^0)$.

Share γ_i and Φ_i with neighbours nodes in N_i through certain agreements.

for $k = 0, 1, 2, 3, \cdots$ do

for every node $i \in V$ do

if $k \in \mathcal{K}_i := \{\kappa_i, 2\kappa_i, 3\kappa_i, \cdots\}$ then

Randomly select a subset $N_i^k \subseteq N_i$ and send request to neighbour nodes in N_i^k .

Employ Algorithm 2 to recover \mathbf{z}_j^k by $\mathbf{z}_j^k = 1 \text{BCS}(\mathbf{w}_j^k, \Phi_j, \gamma_j)$ for each neighbour $j \in N_i^k$.

Generate noise $\boldsymbol{\xi}_i^k \sim \mathcal{N}\left(\mathbf{0}, \varrho_i \mathbf{I}\right)$ and update parameters by $m_i^k = \left|N_i^k\right|, \quad \overline{\mathbf{w}}_i^k = \frac{1}{m_i^k} \sum_{j \in N_i^k} \mathbf{z}_j^k, \quad \mathbf{u}_i^k = \sigma_i m_i^k \overline{\mathbf{w}}_i^k - \nabla f_i(\overline{\mathbf{w}}_i^k), \quad \mathbf{w}_i^{k+1} = \mathbb{P}_{\Omega}\left(\frac{\mathbf{u}_i^k + \boldsymbol{\xi}_i^k}{\sigma_i m_i^k}\right). \tag{3}$ else $m_i^k = m_i^{k-1}, \qquad \mathbf{u}_i^k = \mathbf{u}_i^{k-1}, \qquad \mathbf{w}_i^{k+1} = \mathbb{P}_{\Omega}\left(\frac{\mathbf{u}_i^k + \mu \mathbf{w}_i^k}{\sigma_i m_i^k + \mu}\right). \tag{4}$

noise. A popular mechanism \mathcal{M} to ensure DP of algorithm \mathcal{A} is the Gaussian mechanism,

$$\mathcal{M}(D) = \mathcal{A}(D) + \mathcal{N}\left(0, \frac{2\ln(1.25/\delta)}{\varepsilon^2}\eta^2(\mathcal{A})\right),$$

where $\mathcal{N}(0, \sigma^2)$ denotes a Gaussian distribution with mean zero and variance σ^2 .

III. DFL VIA INEXACT ADM

A. Algorithm Design

To address (SDFL), we solve its personalized version,

$$\min_{\mathbf{W}} \sum_{i \in V} \left(f_i(\mathbf{w}_i) + \frac{\sigma_i}{2} \sum_{j \in N_i} \|\mathbf{w}_i - \mathbf{w}_j\|^2 \right),$$
s.t. $\mathbf{w}_i \in \Omega$. $i \in V$. (5)

where $\sigma_i > 0$. We adopt the inexact alternating direction method (iADM) to solve the above problem. To be more specific, when point $\mathbf{W}^k = \left(\mathbf{w}_1^k, \mathbf{w}_2^k, \cdots, \mathbf{w}_m^k\right)$ is obtained, we update \mathbf{w}_i^{k+1} for $i \in V$ by solving the following problem,

$$\min_{\mathbf{w}_{i} \in \Omega} f_{i}(\mathbf{w}_{i}) + \frac{\sigma_{i}}{2} \sum_{j \in N_{i}^{k}} \|\mathbf{w}_{i} - \mathbf{w}_{j}^{k}\|^{2},$$
 (6)

where $N_i^k \subseteq N_i$ is a randomly selected subset and also contains node i. The overall algorithmic framework is presented in Algorithm 1. We would like to explain why we update \mathbf{w}_i^k by (3) and (4). Let $a \in \{1, 2, 3, \ldots\}$. For each node i, we consider κ_i consecutive iterations:

$$(a-1)\kappa_i+1$$
, $(a-1)\kappa_i+2$, ..., $a\kappa_i-1$, $a\kappa_i$.

• When $k=(a-1)\kappa_i+1, (a-1)\kappa_i+2, \ldots, a\kappa_i-1$ where no communication occurs between node i and its neighbour nodes $j\in N_i^k\equiv N_i^{(a-1)\kappa_i}$, we update \mathbf{w}_i^{k+1} by solving

$$\mathbf{w}_{i}^{k+1} = \underset{\mathbf{w}_{i} \in \Omega}{\operatorname{argmin}} \left\langle \nabla f_{i} \left(\overline{\mathbf{w}}_{i}^{(a-1)\kappa_{i}} \right), \mathbf{w}_{i} \right\rangle$$

$$+ \frac{\sigma_{i}}{2} \sum_{j \in N_{i}^{k}} \left\| \mathbf{w}_{i} - \mathbf{z}_{j}^{(a-1)\kappa_{i}} \right\|^{2} + \frac{\mu}{2} \left\| \mathbf{w}_{i} - \mathbf{w}_{i}^{k} \right\|^{2}$$

$$= \mathbb{P}_{\Omega} \left(\frac{\mathbf{u}_{i}^{(a-1)\kappa_{i}} + \mu \mathbf{w}_{i}^{k}}{\sigma_{i} m_{i}^{(a-1)\kappa_{i}} + \mu} \right), \tag{7}$$

where $\overline{\mathbf{w}}_i^k$ and \mathbf{u}_i^k are defined in (3), and \mathbf{z}_j^k is the recovered version of \mathbf{w}_j^k by node i from node j. This leads to (4). One can observe that for these $\kappa_i - 1$ iterations, $\mathbf{u}_i^{(a-1)\kappa_i}$ is fixed, lessening the computational complexity.

• When $k = a\kappa_i$ where communication occurs between node i and node $j \in N_i^k$, we update \mathbf{w}_i^{k+1} by solving

$$\mathbf{w}_{i}^{k+1} = \underset{\mathbf{w}_{i} \in \Omega}{\operatorname{argmin}} \left\langle \nabla f_{i} \left(\overline{\mathbf{w}}_{i}^{k} \right) - \boldsymbol{\xi}_{i}^{k}, \mathbf{w}_{i} \right\rangle + \frac{\sigma_{i}}{2} \sum_{j \in N_{i}^{k}} \left\| \mathbf{w}_{i} - \mathbf{z}_{j}^{k} \right\|^{2}$$
$$= \mathbb{P}_{\Omega} \left(\frac{\mathbf{u}_{i}^{k} + \boldsymbol{\xi}_{i}^{k}}{\sigma_{i} m_{i}^{k}} \right), \tag{8}$$

where ξ_i is the noise which aims to perturb $\nabla f_i(\overline{\mathbf{v}}_i^k)$ so as to ensure the data privacy for node i. This gives rise to updating \mathbf{w}_i^{k+1} by (3).

B. One-bit Compressive Sensing

To ensure the great efficiency of communication among neighbour nodes, our aim is to exchange information in the form of 1-bit data. However, recovering accurate information (i.e., the trained local parameter) from 1-bit observations is quite challenging without additional information. To break through this limitation, we leverage the technique of 1BCS, which involves two phases.

- Phase I: Encoding. Suppose each node i ∈ V has a encoding matrix Φ_i ∈ ℝ^{d_i×n}, where d_i > 0. This coding matrix is only accessible to node i 's neighbours N_i through certain agreements. When a parameter w_j ∈ Ω is trained at node j ∈ N_i, node j encodes it as presented in Algorithm 2, where γ_j > 0 (e.g., 10 or 100) and ⊙ is the Hadamard product. We point out Step 2 in Algorithm 2 aims to rescale w_j so that x_j does not have tiny magnitudes of non-zero entries. It is recognized that small values in the magnitude of w_j can cause failures of many algorithms to recover w_j.
- Phase II: Decoding. After receiving 1-bit signal c_j and length $\|\mathbf{w}_j\|$, node i tries to decode \mathbf{w}_j as presented in Algorithm 2. This is the well-known 1BCS [43]. The decoding process (i.e., solving problem (9)) can be accomplished using a gradient projection subspace pursuit (GPSP) algorithm proposed in [44]. It has been shown in [44], [45] that solution \mathbf{w}_j can be decoded successfully with high probability if Φ_i is a randomly generated Gaussian matrix and d_i exceeds a certain threshold. Moreover, both theoretical and numerical results have demonstrated that the sparser (i.e., the smaller s) solution \mathbf{w}_j , the easier the problem to be solved. This explains why we introduce a sparsity constraint in (DFL).

Algorithm 2: $\mathbf{z}_j = 1 \operatorname{BCS}(\mathbf{w}_j, \mathbf{\Phi}_i, \gamma_j)$

- -- encoding by node j--
- 1. Compute $\|\mathbf{w}_j\|$.
- 2. Let $\mathbf{x}_{j} = \operatorname{sign}\left(\mathbf{w}_{j}\right) \odot \log_{\gamma_{j}}\left(1 + |\mathbf{w}_{j}|\right)$.
- 3. Compress \mathbf{x}_i by $\mathbf{c}_i := \text{sign} \left(\Phi_i \left(\mathbf{x}_i / \| \mathbf{x}_i \| \right) \right)$.
- 4. Send $(\|\mathbf{w}_i\|, \mathbf{c}_i)$ to node *i*.
- -- decoding by node i--
- 5. Find a solution \mathbf{v}_i to

$$\mathbf{c}_j = \operatorname{sign}(\mathbf{\Phi}_i \mathbf{v}), \quad \|\mathbf{v}\|_0 \le s.$$
 (9)

- 6. Compute $\mathbf{v}_j = \operatorname{sign}(\mathbf{v}_j) \odot \left(\gamma_j^{|\mathbf{v}_j|} 1\right)$.
- 7. Let $\mathbf{z}_j = (\|\mathbf{w}_j\| / \|\mathbf{v}_j\|) \mathbf{v}_j$ be an estimator to \mathbf{w}_j .

C. Communication Efficiency

Our approach enhances communication efficiency through two key factors. Firstly, communication among neighbouring nodes N_i only occurs when $k \in \mathcal{K}_i = \{\kappa_i, 2\kappa_i, \cdots\}$, meaning it does not happen at every iteration step. Therefore, a larger κ_i allows node i more steps to update its local parameters, leading to an improved communication efficiency. Such a scheme has been extensively employed in literature [1, 46–51]. Most importantly, as shown in Algorithm 2, only 1-bit signal $\mathbf{c}_j \in \mathbb{R}^{d_i}$ and a positive scalar are transmitted among neighbour nodes, significantly enhancing communication efficiency. Moreover, if we take $d_i < n$, then the signal is a compressed version of $\mathbf{w}_j \in \mathbb{R}^n$, further reducing communication costs. Taking $d_i = n = 10^4$ as an example, transmitting a dense

vector $\mathbf{w} \in \mathbb{R}^n$ with double-precision floating entries directly between two neighbours would need 64×10^4 bits. In contrast, Algorithm 2 only transmits $(64 + 10^4)$ -bit content.

D. Computational Efficiency

While the decoding process in Algorithm 2 for node i may incur some computational cost, it only occurs at step $k \in \mathcal{K}_i$. From [44], the decoding complexity is about $O\left(c_1\left(c_2d_in+d_is^2+s^3\right)\right)$, where c_1 and c_2 are two small integers. In general, $s^2 \leq \min\left\{d_i^2,n\right\}$, thereby the complexity reducing to $O\left(c_1c_2d_in\right)$. If we generate sparse Φ_i with α (e.g. 0.05) percent of entries to be non-zeros for each $i \in V$, then the complexity is further reduced to $O\left(\alpha c_1c_2d_in\right)$. Moreover, as the communication only occurs at $k \in \mathcal{K}_i$, complex items \mathbf{u}_i^k in (3) only need to be computed once for consecutive κ_i iterations. While the computation for \mathbf{w}_i^k is quite cheap, with computational complexity about $O\left(nm_i^k + s\log(s)\right)$.

E. Partial Device Participation and Partial Synchronization

Each node i only selects a subset of neighbour nodes, $N_i^k \subseteq N_i$, for the training at every step, enabling node i to deal with the straggler's effect. Following the approach in [49], node i sets a threshold $t_i \in [1, |N_i|)$ and collects signals from the first t_i responding neighbour nodes to form N_i^k . Once t_i signals are received, node i proceeds without waiting for the remaining nodes, which are considered stragglers for that iteration. In practical applications, a neighbour node j with unreliable and imperfect communication links can be treated as a straggler, indicating that node i should not pick it, i.e., $j \notin N_i^k$. Note that such a strategy is known for partial device participation in centralized FL [52–54].

Moreover, one can observe that Algorithm 1 enables node i to keep using \mathbf{z}_j^k for nodes $j \notin N_i^k$ as these parameters are previously stored at node i. Therefore, node i only needs to wait for signals from nodes N_i^k to synchronize.

Finally, each node i operates with a communication interval κ_i , allowing for asynchronous behavior across different nodes. This flexibility enables each node to control its local training schedule independently.

F. Privacy Guarantee

To ensure privacy protection, we apply the Gaussian mechanism to the gradient computations, adding random noise to achieve differential privacy. Since the raw dataset at each node is accessed only during the gradient calculation, adding noise at this step ensures that the entire algorithm adheres to differential privacy through the post-processing property [42]. Specifically, in each iteration, the computation at node i can be viewed as $h \circ \nabla f_i$, where $\nabla f_i : D_i \to \mathbb{R}^n$ is the gradient step involving the data, and $h : \mathbb{R}^n \to \mathbb{R}^n$ represents subsequent computations in (3) that do not access the data.

We emphasize that this privacy-preserving mechanism not only provides rigorous differential privacy guarantees but also enhances robustness. Robustness, in this context, refers to the model's ability to maintain consistent predictions in the presence of small adversarial perturbations δ to input data \mathbf{x} .

As discussed in [55, 56], the noise magnitude required for achieving a certain level of privacy (characterized by (ϵ, δ)) can be leveraged to provide robustness guarantees.

IV. THEORETICAL ANALYSIS

In this section, we provide a theoretical analysis of our proposed algorithm, including the assumptions, matrix representations, convergence analysis, and privacy guarantees.

A. Convergence analysis

To simplify the convergence analysis, we choose the following parameters.

1) Set $\mathbf{W}^0 = \mathbf{0}$ and let $\kappa_i = k_0$ for any $i \in V$ for simplicity (In fact, we can let k_0 be the least common multiple of $\{\kappa_1, \kappa_2, \ldots, \kappa_m\}$ and then the subsequent analysis remains similar to the case of $\kappa_i = k_0$). This allows us to focus on steps $ak_0, a = 0, 1, 2, 3, \ldots$ Therefore, at ak_0 th step, all nodes communicate with their neighbours. At this moment, we define an average point by

$$\boldsymbol{\varpi}^{ak_0} := \frac{1}{m} \sum_{i=1}^{m} \mathbf{w}_i^{ak_0}.$$
 (10)

2) Set $m_i = m_j$, $\sigma_i = c/t_i$, $m_i^k = t_i$ for $\forall i, j, k$, where c > 0 can be chosen flexibly and $t_i \leq m_i$ is a positive integer.

To build the convergence, we make the following assumptions.

Assumption 1. For every $i \in V$, gradient ∇f_i is Lipschitz continuous with a constant $\ell_i > 0$. Denote $\ell := \max_{i \in V} \ell_i$.

Assumption 2. Let U(V) be a uniform distribution on V. For any \mathbf{w} , $\mathbb{E}_{i \sim \mathcal{U}(V)} \|\nabla f_i(\mathbf{w}) - \frac{1}{m} \sum_{j \in V} \nabla f_j(\mathbf{w})\|^2 \leqslant \zeta^2$.

Assumption 3. *1BCS technique accurately recovers* \mathbf{w}_{i}^{k} .

Noted that Assumptions 1 and 2 are standard in DFL, and Assumption 3 can be justified with high probability [44, 45].

Assumption 4. Let $E^k := \{(i,j) : j \in N_i^k, i \in V\}$ be the set of the selected edges at step k and B be a given integer. Suppose graph

$$G_t^B := \left(V, E^{tk_0} \cup E^{(t+1)k_0} \cup \ldots \cup E^{(t+B)k_0}\right)$$
 (11)

is connected for any $t \in \{0, 1, 2, \ldots\}$.

The above assumption is related to the uniformly strong connection [57] and can be satisfied with a high probability. For example, a sufficient condition to ensure this assumption is that every pair of clients communicates at least once for each B communication rounds, and one can check that this sufficient condition holds with a probability

$$p \ge \prod_{i=1}^{m} \left[1 - \left(1 - \frac{t_i - 1}{m - 1} \right)^B \right]^{m-1},$$

which is relatively high, e.g., $p \approx 1$ when m = 32, $B \ge 20$, and $t_i \ge (m+1)/2$. Assumption 4 allows us to avoid imposing specific conditions on the communication matrix, thereby

increasing its generality and extending its applicability. Finally, letting B>0 given in Assumption 4, we define

$$c_0 := \left(\frac{80m\sqrt{\ell}}{1-\tau}\right)^2, \ \tau := \left(1 - \frac{1}{m^{mB}}\right)^{\frac{1}{B}}.$$
 (12)

It is clear that $\tau \in (0,1)$. When $\mathbf{w}_1 = \cdots = \mathbf{w}_m$, we write

$$f(\mathbf{w}) := \sum_{i \in V} f_i(\mathbf{w}).$$

Theorem 1. Under Assumptions 1 to 4 and setting $c \ge c_0$, the following bound holds for Algorithm 1,

$$\frac{1}{T} \sum_{a=0}^{T-1} \mathbb{E} \left\| \nabla f \left(\boldsymbol{\varpi}^{ak_0} \right) \right\|^2 \leq \frac{8mc(f(0) - f^*)}{T} + \frac{m^2 c_0 \zeta^2 + 16mck_0 e_{\infty}}{c}$$

where $\varrho := \sum_{i=1}^{m} \varrho_i$ and e_{∞} is an error bound relied on the sparse projection of each iteration and the added noise.

Proof. The detailed proof is presented in Appendix A-C (available in supplemental material).

In the above theorem, the upper bound of the error consists of three components. The second error term, $c_0m^2\zeta^2/c$, arises from sampling to select neighbour nodes. The third error term, $16mk_0e_\infty$, is due to the sparse projection and the added noise for privacy preservation. The detailed formulation of e_∞ is provided in Lemma 2 in the Appendix.

B. Privacy Guarantee

We now demonstrate that our algorithm provides differential privacy guarantees at each iteration as well as the entire process for datasets D_1, D_2, \ldots, D_m . Hereafter, we set

$$\varrho_i := \frac{2\ln(1.25/\delta)u_i^2}{\varepsilon^2}, \quad i \in \mathcal{V}, \tag{13}$$

and consider the algorithm as a query process $\mathcal{A}: D \to \mathbb{R}^n$, where $D = (D_1, D_2, \dots, D_m)$ represents the collection of all local datasets, and D_i is the data of node i. Moreover, we need the following condition that has been frequently assumed in differential privacy analysis [13, 17, 18].

Assumption 5. $\|\nabla f_i(\mathbf{w})\| \le u_i/2$ for any \mathbf{w} and any $i \in V$.

Here we point out that the existing literature considering DP in decentralized FL only gives a privacy guarantee in each iteration, such as [52]. Instead, we give the privacy guarantee by viewing the algorithm as a whole part, which is more realistic for various applications.

Theorem 2. Given $\varepsilon > 0, \delta \in (0,1)$, each step of Algorithm 1 achieves (ε, δ) -differential privacy under Assumption 5.

Proof. The detailed proof is presented in Appendix D (available in supplemental material).

Theorem 3. Given $\varepsilon > 0, \delta \in (0,1)$, Algorithm 1 with ak_0 total iterations achieves

$$\left(\sqrt{2a\ln\left(1/\delta\right)}\varepsilon + a\varepsilon\left(e^{\varepsilon} - 1\right), (a+1)\delta\right) -$$

differentially privacy under Assumption 5.

Proof. The detailed proof is presented in Appendix E (available in supplemental material). \Box

V. NUMERICAL EXPERIMENTS

In this section, we present numerical experiments to evaluate the performance of CEPS. All experiments are implemented using MATLAB (R2021b) on a laptop with 32GB memory and 3.7GHz CPU.

A. Testing Example

Example 1. (Linear Regression). Consider a linear regression problem where each node $i \in V$ has an objective function

$$f_i(\mathbf{w}) = \frac{1}{2m_i} \|\mathbf{A}_i \mathbf{w} - \mathbf{b}_i\|^2,$$

where $\mathbf{b}_i \in \mathbb{R}^{m_i}$ and $\mathbf{A}_i \in \mathbb{R}^{m_i \times n}$ is a random Gaussian matrix. To assess the effectiveness of CEPS, we assume there is a 'ground truth' solution $\mathbf{w}^* \in \mathbb{R}^n$ with s non-zeros entries. Then $\mathbf{b}_i := \mathbf{A}_i \mathbf{w}^* + 0.5 \mathbf{e}_i$, where \mathbf{e}_i is the noise. All entries of \mathbf{A}_i and \mathbf{e}_i are identically and independently distributed from a standard normal distribution, while the non-zero entries of \mathbf{w}^* are uniformly generated from $[0.5, 2] \cup [-2, -0.5]$.

Example 2. (Logistic Regression). Consider a logistic regression problem where each node i has an objective function

$$f_i(\mathbf{w}) = \frac{1}{m_i} \sum_{t=1}^{m_i} \left(\ln \left(1 + e^{\left\langle \mathbf{a}_i^t, \mathbf{w} \right\rangle} \right) - b_i^t \left\langle \mathbf{a}_i^t, \mathbf{w} \right\rangle \right) + \frac{\lambda}{2} \|\mathbf{w}\|^2,$$

where $\mathbf{a}_i^t \in \mathbb{R}^n$, $b_i^t \in \{0,1\}$, and $\lambda > 0$ is a penalty parameter (e.g., $\lambda = 0.001$ in our numerical experiments). We use two real datasets: 'qot' (Qsar oral toxicity) from UCI [58] and 'rls' (real-sim) from Libsvm [59] to generate \mathbf{a}_i and b_i . The dimensions of two datasets are (m,n) = (1024,8992) and (m,n) = (20958,72309). The samples are randomly divided into m groups, corresponding to m nodes.

B. Implementations

The basic setup for CEPS in Algorithm 1 is given as follows. We begin by randomly generating a graph and obtain $\{N_i:i\in V\}$. For each node $i\in V$, we randomly select subset N_i^k such that $t_i=\left|N_i^k\right|=r\left|N_i\right|$, where $r\in(0,1]$ is the participation rate. Encoding matrix $\mathbf{\Phi}_i\in\mathbb{R}^{d_i\times n}$ is generated similarly to \mathbf{A}_i with $d_i=n/2$. Other parameters are initialized as $\gamma_i=5,\ \mu=0.1,\ \sigma_i=\lambda_{\max}\left(\mathbf{A}_i^{\top}\mathbf{A}_i\right)/\left(m(2r+0.1)d_i\right)$, where $\lambda_{\max}(\mathbf{A})$ stands for the largest eigenvalue of \mathbf{A} , and κ_i is randomly chosen from [10,15]. The privacy constants in (13) are set as $\delta=0.5,\ u_i=0.1,\ \mathrm{and}\ \varepsilon\in[0.1,1]$. Finally, we terminate the algorithm if

$$\frac{1}{sm} \left\| \mathbf{W}^k - (\boldsymbol{\varpi}^k, \cdots, \boldsymbol{\varpi}^k) \right\|^2 \le \text{tol},$$

where tol = 0.005 if no DP techniques are used in CEPS (i.e., $\varrho_i = 0$) and tol = 0.0025/ ε otherwise.

TABLE II: Four variants of CEPS.

	1BCS	No 1BCS
DP	DP-1BCS	DP-Perf
No DP	NoDP-1BCS	NoDP-Perf

TABLE III: Self-Comparison of CEPS.

-	m				ε			r		
	32	64	128	0.25	0.50	0.75	0.20	0.50	0.80	
				Objective						
DP-1BCS	0.127	0.125	0.125	0.129	0.126	0.126	0.127	0.127	0.129	
NoDP-1BCS	0.126	0.125	0.125	0.127	0.126	0.126	0.126	0.127	0.130	
DP-Perf	0.127	0.125	0.125	0.129	0.126	0.126	0.126	0.130	0.131	
NoDP-Perf	0.126	0.125	0.125	0.127	0.125	0.125	0.126	0.126	0.133	
				Tim	e (seco	nds)				
DP-1BCS	1.225	3.689	14.20	1.101	1.322	1.432	1.224	2.412	2.713	
NoDP-1BCS	1.105	3.551	13.72	1.095	1.171	1.179	1.086	2.292	2.607	
DP-Perf	0.269	0.587	1.211	0.290	0.287	0.300	0.282	0.290	0.287	
NoDP-Perf	0.286	0.589	1.195	0.283	0.294	0.304	0.295	0.291	0.291	
				Iterations						
DP-1BCS	32	30	30	30	32	35	32	30	26	
NoDP-1BCS	29	29	29	29	29	29	29	29	23	
DP-Perf	28	28	28	28	30	32	28	28	24	
NoDP-Perf	27	25	27	27	27	27	27	27	21	

C. Self-comparison of CEPS

To assess the performance of the 1BCS and DP techniques in Algorithm 2, we compare four variants of CEPS with and without using these two techniques. As shown in Table II, 'Perf' stands for perfect communication (i.e., without 1BCS). That is, $\mathbf{z}_j^k = 1\mathrm{BCS}\left(\mathbf{w}_j^k, \mathbf{\Phi}_i, \gamma_j\right)$ is replaced by $\mathbf{z}_j^k = \mathbf{w}_j^k$ for every $j \in N_i^k$ in Algorithm 2. 'No DP' means no noise added in (3), namely $\varrho_i = 0$. Therefore, 'DP-Perf' represents CEPS with DP but without 1BCS, and 'NoDP-Perf' represents CEPS without DP and 1BCS. For Example 1, we set n=1000 and s=10 and generate each $m_i \in [250,750], i \in V$ to see the impact of node number m, noisy ratio ε , and participation rate r on the convergence performance of CEPS.

1) Effect of m. Fig. 1 illustrates the effect of varying $m \in \{32, 64, 128\}$ by fixing $(\varepsilon, r) = (0.5, 0.2)$. For fewer nodes (e.g., m = 32), DP-1BCS requires more iterations to achieve the optimal function values. As the number of nodes increases, the performance differences among the four CEPS variations diminish. From Table III, no significant differences are observed in objective values or iteration counts among the four algorithms. However, it is evident that as m increases, the computational time also rises.

2) Effect of ε . Fig. 2 demonstrates the effect of altering $\varepsilon \in \{0.25, 0.5, 0.75\}$ by fixing (m,r)=(32,0.2). According to (3), smaller ε introduces more noise to perturb the transmitted messages. This enhances privacy but also results in noticeable fluctuations during the training process, as observed in the figure. For $\varepsilon=0.25$, NoDP-1BCS and NoDP-Perf exhibit much smoother behavior compared to DP-1BCS and DP-Perf. As ε increases (e.g., $\varepsilon \geq 0.5$), the objective function values of all four algorithms follow a similar declining trend, indicating that the impact of noise becomes negligible. From

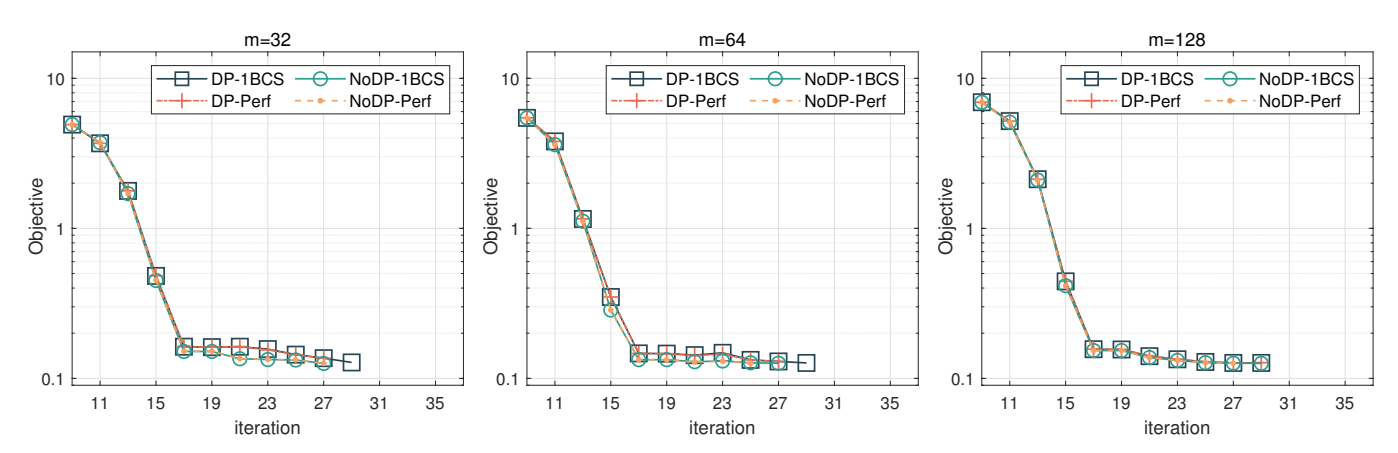


Fig. 1: Self-comparison of CEPS: Effect of m.

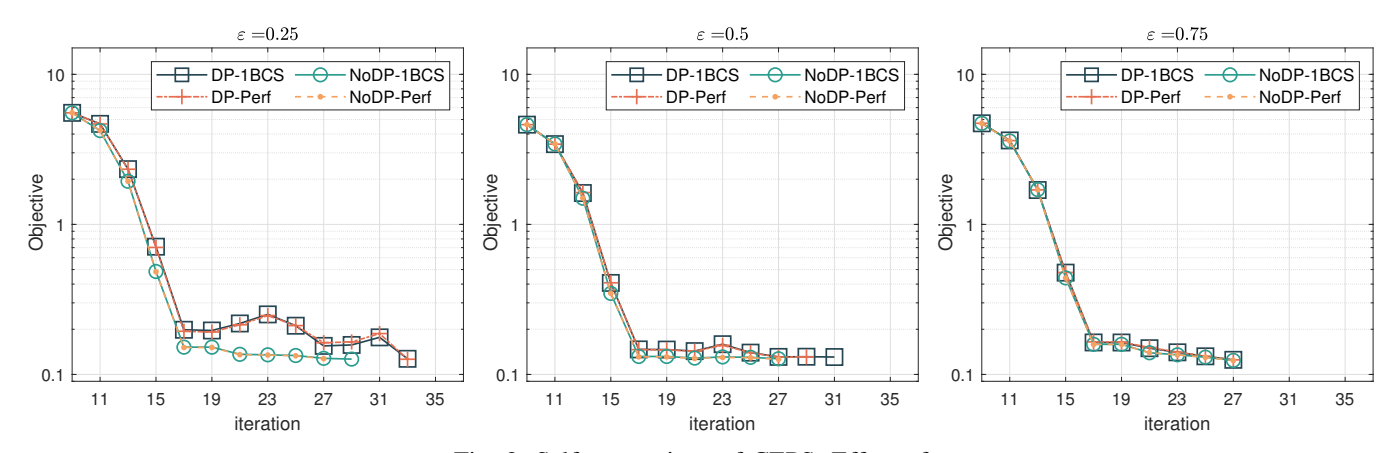


Fig. 2: Self-comparison of CEPS: Effect of ε .

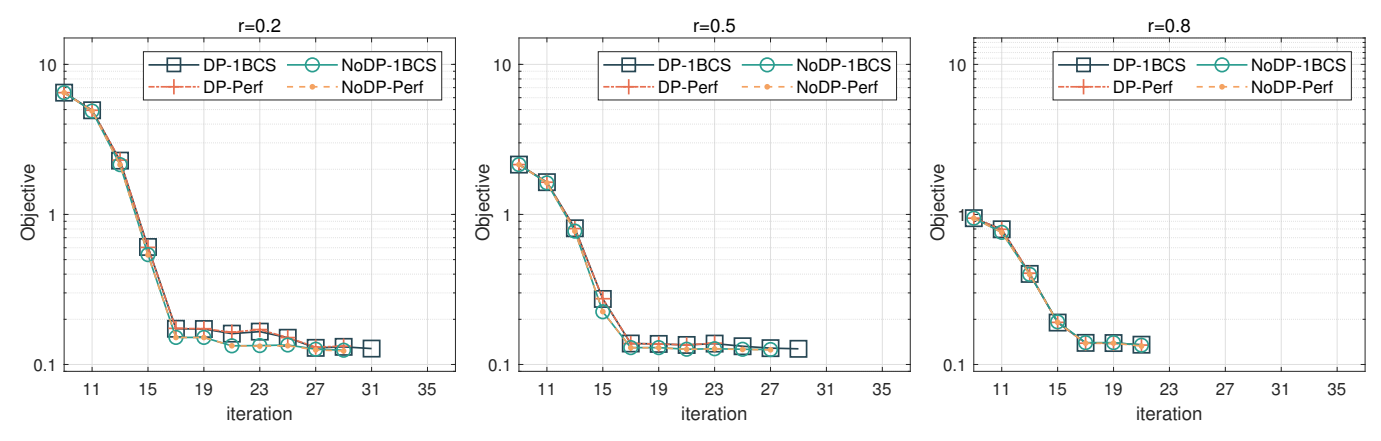


Fig. 3: Self-comparison of CEPS: Effect of r.

Table III, no significant differences are observed in objective values. However, more iterations and time are required for DP-1BCS and DP-Perf when ε decreases.

3) Effect of r. Fig. 3 presents the effect of changing $r \in \{0.2, 0.5, 0.8\}$ by fixing $(m, \varepsilon) = (32, 0.5)$. It appears that the range of $r \in [0.2, 0.8]$ has minimal impact on the convergence of these four variants, as the produced curves closely coincide. From Table III, their generated objective function values are comparable. However, as more neighbour modes are selected (i.e., as r increases), the computational time increases while the number of iterations decreases.

D. Comparison with other federated learning methods

We evaluate the performance of CEPS under two communication scenarios: ideal communication (CEPS-Perf) and communication using 1BCS (CEPS-1BCS) by comparing them with D-PSGD [5], DFedAvgM [8], and DFedSAM [9]. Additionally, we also introduce two variants of D-PSGD: D-PSGD-DN and D-PSGD-PC. The former uses a dynamic mixing matrix network and the latter employs partial communication. To ensure fair comparison, all algorithms perform communication among nodes every 10 iterations. Finally, for

D-PSGD and D-PSGD-DN, each node imposes all neighbours to join in training, while for the other five methods, each node selects $r|N_i|$ neighbour nodes to participate. We now assess the performance of these methods on Examples 1 and 2.

4) Effect of m. Fig. 4 illustrates the convergence behavior for Example 1 as the number of clients, m, varies over {32,64,128}. Generally, increasing the number of communication nodes reduces the required communication rounds. Notably, CEPS consistently requires the fewest communication rounds to converge across all scenarios. Plain D-PSGD converges second fastest, benefiting from the participation of all clients. Incorporating a dynamic network in D-PSGD-DN has only a minor impact on convergence speed. In contrast, partial communication in D-PSGD-PC results in slower convergence. While both DFedAvgM and DFedSAM outperform D-PSGD-PC, neither matches the performance of CEPS, which achieves the fastest convergence overall.

Figs. 5-7 provide additional numerical performance metrics, including communication rounds (CR), data transmission volume (DTV), and computational time. The left column shows results for Example 1, the middle column corresponds to Example 2 using the 'qot' dataset, and the right column presents results for the 'rls' dataset. Fig. 5 presents the expected trend: increasing m generally leads to fewer CR. Once again, CEPS outperforms all other methods across all scenarios. Fig. 6 highlights the communication efficiency of CEPS-1BCS during training. Compared to all other methods, it achieves a substantial reduction in data transmission volume, saving at least 90% of the communication overhead. Even without 1BCS, CEPS-Perf still outperforms the other methods in terms of DTV. Fig. 7 compares the computational time across the seven methods. CEPS-1BCS achieves faster computation compared to DFedAvgM and DFedSAM, although its computational time is slightly higher than that of D-PSGD. However, it is important to note that the reported time does not include communication time. In practical applications, communication time is typically much more expensive than the computational time. As a result, CEPS-1BCS remains highly competitive, as evidenced by the reduced CR shown in Fig. 5. Additionally, CEPS-Perf consistently consumes the shortest computational time across all scenarios.

- 5) Effect of ε . To see such an effect, we employ all methods to solve Example 1 by fixing (m,n,r)=(64,1000,0.2) but altering $\varepsilon\in\{0.5,1,2\}$. The results are presented in Table IV. One can observe that when ε is small (i.e. the privacy budget is low), all the methods are impacted by the noise. Specifically, all D-PSGD variants fail to converge when $\varepsilon=0.5$. However, as ε increases, all methods show improved performance. Evidently, CEPS yields the best results across all settings.
- 6) Effect of r. Again for Example 1, we fix $(m,n,\varepsilon)=(64,1000,2)$ but vary $r\in\{0.2,0.5,0.8\}$. The results are reported in Table V. Generally, increasing r leads to fewer iterations but higher DTV. This is expected, as a higher participation rate incorporates more clients into the communication network, thereby increasing communication overhead. As always, CEPS stands out among all methods, maintaining relative stability while consistently achieving the highest communication efficiency.

TABLE IV: Comparison of ε .

	$\varepsilon = 0.5$			$\varepsilon = 1$			$\varepsilon = 2$		
	Obj	Iter	Time	Obj	Iter	Time	Obj	Iter	Time
CEPS-Perf	0.124	24	1.038	0.123	22	1.062	0.123	22	1.026
CEPS-1BCS	0.123	24	2.997	0.123	22	3.111	0.123	22	2.161
DPSGD	-*	-	-	0.561	41	2.692	0.129	81	3.872
DPSGD-DN	-	-	-	0.192	71	3.509	0.129	91	4.114
DPSGD-PC	-	-	-	0.185	81	3.805	0.132	101	4.492
DFedAvgM	0.577	51	2.911	0.274	61	3.289	0.156	91	4.199
DFedSAM	0.636	41	3.221	0.243	61	4.049	0.150	81	4.914

^{* &#}x27;-' means that the algorithm diverges.

TABLE V: Comparison of r.

	r = 0.2			r = 0.5			r = 0.8		
	Obj	Iter	DTV*	Obj	Iter	DTV	Obj	Iter	DTV
CEPS-1BCS	0.126	38	0.78	0.126	28	1.36	0.126	26	2.05
CEPS-Perf	0.126	28	3.65	0.126	28	9.13	0.126	24	12.52
NoDP-1BCS	0.126	29	0.63	0.126	29	1.44	0.127	23	1.95
NoDP-Perf	0.125	29	3.78	0.125	27	8.80	0.125	21	10.96
DPSGD-PC	0.131	81	13.27	0.128	61	24.99	0.128	51	33.42
DFedAvgM	0.140	61	9.99	0.128	51	20.89	0.133	31	20.32
DFedSAM	0.151	61	9.99	0.166	51	20.89	0.208	31	20.32

^{*}The unit of DTV is 106 bytes.

VI. CONCLUSION

This paper introduces a novel algorithm, CEPS, for SDFL. By addressing critical challenges such as communication overhead, computational efficiency, robustness against stragglers, and privacy protection, CEPS provides a promising solution to improve the performance of DFL systems. By integrating the 1BCS technique, the algorithm significantly reduces communication rounds and data transmission, setting it apart from existing approaches. Moreover, CEPS leverages closed-form solutions for computational efficiency and incorporates the Gaussian mechanism for rigorous privacy protection. The theoretical convergence guarantee and numerical experiments further validate its effectiveness. Overall, CEPS stands as a promising approach for SDFL, particularly in challenging communication environments.

REFERENCES

- B. McMahan, E. Moore, D. Ramage, S. Hampson, and B. Aguera y Arcas, "Communication-efficient learning of deep networks from decentralized data," in *Artif. Intell. Stat.* PMLR, 2017, pp. 1273–1282.
- [2] P. Kairouz, H. B. McMahan, B. Avent, A. Bellet, M. Bennis, A. N. Bhagoji, K. Bonawitz, Z. Charles, G. Cormode, R. Cummings *et al.*, "Advances and open problems in federated learning," *Found. Trends Mach. Learn.*, vol. 14, no. 1–2, pp. 1–210, 2021.
- [3] E. T. M. Beltrán, M. Q. Pérez, P. M. S. Sánchez, S. L. Bernal, G. Bovet, M. Gil, G. Martínez, and A. H. Celdrán, "Decentralized federated learning: Fundamentals, state of the art, frameworks, trends, and challenges," *IEEE Commun. Surv. Tutor.*, 2023.

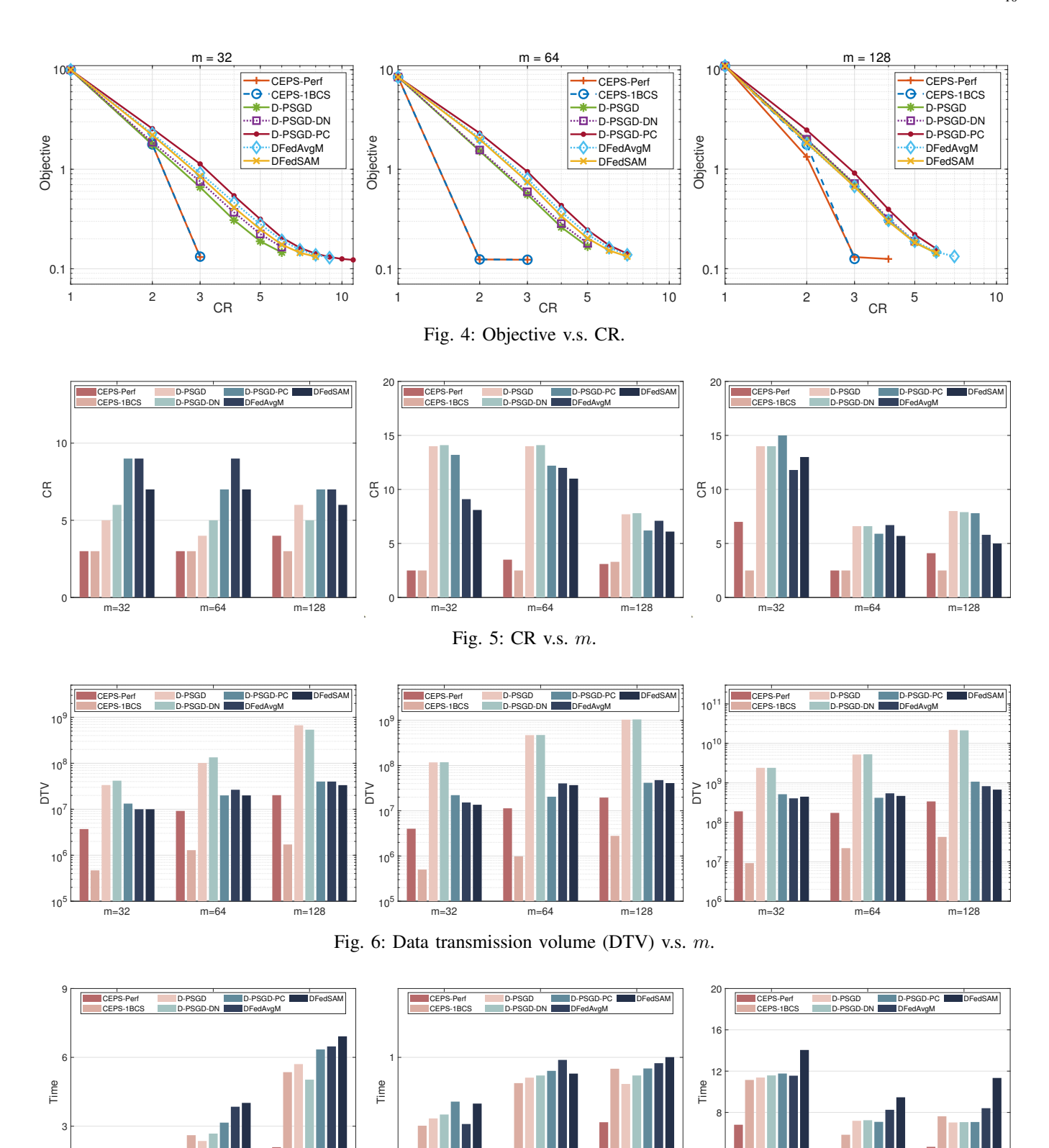


Fig. 7: Time v.s. m.

- [4] L. Yuan, Z. Wang, L. Sun, S. P. Yu, and C. G. Brinton, "Decentralized federated learning: A survey and perspective," *IEEE Internet Things J.*, 2024.
- [5] X. Lian, C. Zhang, H. Zhang, C.-J. Hsieh, W. Zhang, and J. Liu, "Can decentralized algorithms outperform centralized algorithms? a case study for decentralized

- parallel stochastic gradient descent," Adv. Neural Inf. Process. Syst., vol. 30, 2017.
- [6] V. Mothukuri, R. M. Parizi, S. Pouriyeh, Y. Huang, A. Dehghantanha, and G. Srivastava, "A survey on security and privacy of federated learning," *Future Gener. Comput. Syst.*, vol. 115, pp. 619–640, 2021.
- [7] H. Tang, S. Gan, C. Zhang, T. Zhang, and J. Liu, "Communication compression for decentralized training," *Adv. Neural Inf. Process. Syst.*, vol. 31, 2018.
- [8] T. Sun, D. Li, and B. Wang, "Decentralized federated averaging," *IEEE Trans. Pattern Anal. Mach. Intell.*, vol. 45, no. 4, pp. 4289–4301, 2022.
- [9] Y. Shi, L. Shen, K. Wei, Y. Sun, B. Yuan, X. Wang, and D. Tao, "Improving the model consistency of decentralized federated learning," in *Int. Conf. Mach. Learn*. PMLR, 2023, pp. 31 269–31 291.
- [10] J. Wang, A. K. Sahu, Z. Yang, G. Joshi, and S. Kar, "Matcha: Speeding up decentralized sgd via matching decomposition sampling," in *Indian Control Conf.* IEEE, 2019, pp. 299–300.
- [11] J. Bayrooti, Z. Gao, and A. Prorok, "Differentially private decentralized deep learning with consensus algorithms," *arXiv preprint arXiv:2306.13892*, 2023.
- [12] A. Lalitha, S. Shekhar, T. Javidi, and F. Koushanfar, "Fully decentralized federated learning," in Workshop Bayesian Deep Learn. (NeurIPS), vol. 2, 2018.
- [13] C. Pappas, D. Chatzopoulos, S. Lalis, and M. Vavalis, "Ipls: A framework for decentralized federated learning," in *IFIP Netw. Conf.* IEEE, 2021, pp. 1–6.
- [14] H. Ye, L. Liang, and G. Y. Li, "Decentralized federated learning with unreliable communications," *IEEE J. Sel. Top. Signal Process.*, vol. 16, no. 3, pp. 487–500, 2022.
- [15] C. Li, G. Li, and P. K. Varshney, "Decentralized federated learning via mutual knowledge transfer," *IEEE Internet Things J.*, vol. 9, no. 2, pp. 1136–1147, 2021.
- [16] S. Kalra, J. Wen, J. C. Cresswell, M. Volkovs, and H. R. Tizhoosh, "Decentralized federated learning through proxy model sharing," *Nat. Commun.*, vol. 14, no. 1, p. 2899, 2023.
- [17] W. Liu, L. Chen, and W. Zhang, "Decentralized federated learning: Balancing communication and computing costs," *IEEE Trans. Signal Inf. Process. Netw.*, vol. 8, pp. 131–143, 2022.
- [18] A. Koloskova, S. Stich, and M. Jaggi, "Decentralized stochastic optimization and gossip algorithms with compressed communication," in *Int. Conf. Mach. Learn.* PMLR, 2019, pp. 3478–3487.
- [19] A. Koloskova, T. Lin, S. U. Stich, and M. Jaggi, "Decentralized deep learning with arbitrary communication compression," in *Int. Conf. Learn. Represent.*, 2020.
- [20] R. Dai, L. Shen, F. He, X. Tian, and D. Tao, "Dispfl: Towards communication-efficient personalized federated learning via decentralized sparse training," in *Int. Conf. Mach. Learn.* PMLR, 2022, pp. 4587–4604.
- [21] Z. Tang, S. Shi, B. Li, and X. Chu, "Gossipfl: A decentralized federated learning framework with sparsified and adaptive communication," *IEEE Trans. Parallel Distrib. Syst.*, vol. 34, no. 3, pp. 909–922, 2022.

- [22] I. Hegedűs, G. Danner, and M. Jelasity, "Gossip learning as a decentralized alternative to federated learning," in *Distrib. Appl. Interoperable Syst.: Proc. 19th IFIP Int. Conf. DAIS 2019.* Springer, 2019, pp. 74–90.
- [23] —, "Decentralized learning works: An empirical comparison of gossip learning and federated learning," *J. Parallel Distrib. Comput.*, vol. 148, pp. 109–124, 2021.
- [24] L. Zhu, Z. Liu, and S. Han, "Deep leakage from gradients," *Adv. Neural Inf. Process. Syst.*, vol. 32, 2019.
- [25] Y. Huang, S. Gupta, Z. Song, K. Li, and S. Arora, "Evaluating gradient inversion attacks and defenses in federated learning," *Adv. Neural Inf. Process. Syst.*, vol. 34, pp. 7232–7241, 2021.
- [26] R. Hu, Y. Guo, H. Li, Q. Pei, and Y. Gong, "Personalized federated learning with differential privacy," *IEEE Internet Things J.*, vol. 7, no. 10, pp. 9530–9539, 2020.
- [27] M. H. u. Rehman, A. M. Dirir, K. Salah, E. Damiani, and D. Svetinovic, "Trustfed: A framework for fair and trustworthy cross-device federated learning in iiot," *IEEE Trans. Ind. Informat.*, vol. 17, no. 12, pp. 8485–8494, 2021.
- [28] M. Ali, F. Naeem, M. Tariq, and G. Kaddoum, "Federated learning for privacy preservation in smart healthcare systems: A comprehensive survey," *IEEE J. Biomed. Health Inform.*, vol. 27, no. 2, pp. 778–789, 2022.
- [29] K. Wei, J. Li, M. Ding, C. Ma, H. H. Yang, F. Farokhi, S. Jin, T. Q. S. Quek, and H. V. Poor, "Federated learning with differential privacy: Algorithms and performance analysis," *IEEE Trans. Inf. Forensics Secur.*, vol. 15, pp. 3454–3469, 2020.
- [30] M. Naseri, J. Hayes, and E. De Cristofaro, "Local and central differential privacy for robustness and privacy in federated learning," arXiv preprint arXiv:2009.03561, 2020
- [31] M. Ryu and K. Kim, "Differentially private federated learning via inexact admm with multiple local updates," *arXiv preprint arXiv:2202.09409*, 2022.
- [32] A. Lowy and M. Razaviyayn, "Private stochastic optimization with large worst-case lipschitz parameter: Optimal rates for (non-smooth) convex losses and extension to non-convex losses," in *Int. Conf. Algorithmic Learn. Theory.* PMLR, 2023, pp. 986–1054.
- [33] Y. Wang and T. Başar, "Decentralized nonconvex optimization with guaranteed privacy and accuracy," *Automatica*, vol. 150, p. 110858, 2023.
- [34] Y. Wang and A. Nedić, "Tailoring gradient methods for differentially private distributed optimization," *IEEE Trans. Autom. Control*, vol. 69, no. 2, pp. 872–887, 2023.
- [35] S. Zhou, K. Xu, and G. Y. Li, "Communication-efficient decentralized federated learning via one-bit compressive sensing," in 2024 IEEE 99th Vehicular Technology Conference (VTC2024-Spring). IEEE, 2024, pp. 1–5.
- [36] E. J. Candes and T. Tao, "Decoding by linear programming," *IEEE tran. inform. theory*, vol. 51, no. 12, pp. 4203–4215, 2005.
- [37] D. L. Donoho, "Compressed sensing," *IEEE Tran. informa. theory*, vol. 52, no. 4, pp. 1289–1306, 2006.
- [38] F. Bach, R. Jenatton, J. Mairal, G. Obozinski et al.,

- "Optimization with sparsity-inducing penalties," *Found. Trends Mach. Learn.*, vol. 4, no. 1, pp. 1–106, 2012.
- [39] R. G. Baraniuk, E. Candes, M. Elad, and Y. Ma, "Applications of sparse representation and compressive sensing [scanning the issue]," *Proc. IEEE*, vol. 98, no. 6, pp. 906–909, 2010.
- [40] S. Zhou, N. Xiu, and H.-D. Qi, "Global and quadratic convergence of newton hard-thresholding pursuit," *J. Mach. Learn. Res.*, vol. 22, no. 12, pp. 1–45, 2021.
- [41] C. Dwork, F. McSherry, K. Nissim, and A. Smith, "Calibrating noise to sensitivity in private data analysis," in *Theory of Cryptography: Third Theory of Cryptography Conference.* Springer, 2006, pp. 265–284.
- [42] M. Abadi, A. Chu, I. Goodfellow, H. B. McMahan, I. Mironov, K. Talwar, and L. Zhang, "Deep learning with differential privacy," in *Proc. 2016 ACM SIGSAC Conf. Comput. Commun. Secur.*, 2016, pp. 308–318.
- [43] P. T. Boufounos and R. G. Baraniuk, "1-bit compressive sensing," in *Conf. Inf. Sci. Syst.* IEEE, 2008, pp. 16–21.
- [44] S. Zhou, Z. Luo, N. Xiu, and G. Y. Li, "Computing one-bit compressive sensing via double-sparsity constrained optimization," *IEEE Trans. Signal Process.*, vol. 70, pp. 1593–1608, 2022.
- [45] L. Jacques, J. N. Laska, P. T. Boufounos, and R. G. Baraniuk, "Robust 1-bit compressive sensing via binary stable embeddings of sparse vectors," *IEEE Trans. Inf. Theory*, vol. 59, no. 4, pp. 2082–2102, 2013.
- [46] S. Zheng, Q. Meng, T. Wang, W. Chen, N. Yu, Z. Ma, and T.-Y. Liu, "Asynchronous stochastic gradient descent with delay compensation for distributed deep learning," arXiv preprint arXiv:1609.08326, 2016.
- [47] H. Yu, S. Yang, and S. Zhu, "Parallel restarted sgd with faster convergence and less communication: Demystifying why model averaging works for deep learning," in *Proc. AAAI Conf. Artif. Intell.*, vol. 33, no. 1, 2019, pp. 5693–5700.
- [48] J. Wang and G. Joshi, "Cooperative sgd: A unified framework for the design and analysis of local-update sgd algorithms," *J. Mach. Learn. Res.*, vol. 22, no. 213, pp. 1–50, 2021.
- [49] X. Li, K. Huang, W. Yang, S. Wang, and Z. Zhang, "On the convergence of fedavg on non-iid data," *arXiv* preprint arXiv:1907.02189, 2019.
- [50] T. Li, A. K. Sahu, M. Zaheer, M. Sanjabi, A. Talwalkar, and V. Smith, "Federated optimization in heterogeneous networks," *Proc. Mach. Learn. Syst.*, vol. 2, pp. 429–450, 2020.
- [51] S. Zhou and G. Y. Li, "Fedgia: An efficient hybrid algorithm for federated learning," *IEEE Trans. Signal Process.*, vol. 71, pp. 1493–1508, 2023.
- [52] Y. Li, T.-H. Chang, and C.-Y. Chi, "Secure federated averaging algorithm with differential privacy," in *IEEE Int. Workshop Mach. Learn. Signal Process.* IEEE, 2020, pp. 1–6.
- [53] S. Zhou and G. Y. Li, "Federated learning via inexact admm," *IEEE Trans. Pattern Anal. Mach. Intell.*, vol. 45, no. 8, pp. 9699–9708, 2023.
- [54] Y. Li, S. Wang, T.-H. Chang, and C.-Y. Chi, "Federated

- stochastic primal-dual learning with differential privacy," *arXiv preprint arXiv:2204.12284*, 2022.
- [55] M. Lecuyer, V. Atlidakis, R. Geambasu, D. Hsu, and S. Jana, "Certified robustness to adversarial examples with differential privacy," in *IEEE Symp. Secur. Privacy*. IEEE, 2019, pp. 656–672.
- [56] H. Asi, J. Ullman, and L. Zakynthinou, "From robustness to privacy and back," in *Int. Conf. Mach. Learn*. PMLR, 2023, pp. 1121–1146.
- [57] A. Nedić and A. Olshevsky, "Distributed optimization over time-varying directed graphs," *IEEE Trans. Autom. Control*, vol. 60, no. 3, pp. 601–615, 2014.
- [58] A. Asuncion, D. Newman *et al.*, "Uci machine learning repository," 2007.
- [59] C.-C. Chang and C.-J. Lin, "Libsvm: a library for support vector machines," *ACM Trans. Intell. Syst. Technol.*, vol. 2, no. 3, pp. 1–27, 2011.

APPENDIX

A. Basic Inequalities

Under gradient Lipschitz assumption, for any w, v we have

$$f_i(\mathbf{w}) \le f_i(\mathbf{v}) + \langle \nabla f_i(\mathbf{v}), \mathbf{w} - \mathbf{v} \rangle + \frac{\ell}{2} \|\mathbf{w} - \mathbf{v}\|^2, \quad (14)$$

and the same rule applies for f with $m\ell$. For any \mathbf{w}_i and t>0

$$\begin{aligned} & \| \sum_{i=1}^{m} \mathbf{w}_{i} \| \leq \sum_{i=1}^{m} \| \mathbf{w}_{i} \|, \ \| \sum_{i=1}^{m} \mathbf{w}_{i} \|^{2} \leq m \sum_{i=1}^{m} \| \mathbf{w}_{i} \|^{2}, \\ & 2 \left\langle \mathbf{w}_{1}, \mathbf{w}_{2} \right\rangle \leq t \| \mathbf{w}_{1} \|^{2} + \frac{1}{t} \| \mathbf{w}_{2} \|^{2}, \end{aligned}$$

$$\|\mathbf{w}_1 + \mathbf{w}_2\|^2 \le (1+t) \|\mathbf{w}_1\|^2 + (1+1/t) \|\mathbf{w}_2\|^2$$
. (15)

To analyze the algorithm globally, we define matrix $\mathbf{A}^k \in \mathbb{R}^{m \times m}$ to represent the communication topology by

$$\mathbf{A}_{ji}^{k} := \begin{cases} \frac{1}{t_{i}} & \text{if } j \in N_{i}^{k}, \\ 0 & otherwise, \end{cases}$$
 (16)

and further define matrices \mathbf{W}^k , $\overline{\mathbf{W}}^k$, $\mathbf{\Psi}^k$, $\mathbf{\Xi}^k \in \mathbb{R}^{n \times m}$ to represent the collection of local models, mixed models, gradients, and noise terms at step k:

$$\mathbf{W}^{k} := (\mathbf{w}_{1}^{k}, \mathbf{w}_{2}^{k}, \cdots, \mathbf{w}_{m}^{k}),$$

$$\overline{\mathbf{W}}^{k} := (\overline{\mathbf{w}}_{1}^{k}, \overline{\mathbf{w}}_{2}^{k}, \cdots, \overline{\mathbf{w}}_{m}^{k}) = \mathbf{W}^{k} \mathbf{A}^{k},$$

$$\mathbf{\Psi}^{k} := (\nabla f_{1}(\overline{\mathbf{w}}_{1}^{k}), \nabla f_{2}(\overline{\mathbf{w}}_{2}^{k}), \cdots \nabla f_{m}(\overline{\mathbf{w}}_{m}^{k})),$$

$$\mathbf{\Xi}^{k} := (\boldsymbol{\xi}_{1}^{k}, \boldsymbol{\xi}_{2}^{k}, \cdots, \boldsymbol{\xi}_{m}^{k}).$$
(17)

By the definition of average point

$$\boldsymbol{\varpi}^{ak_0} := \frac{1}{m} \sum_{i=1}^{m} \mathbf{w}_i^{ak_0}, \tag{18}$$

we have

$$\boldsymbol{\varpi}^{\alpha} = \frac{1}{m} \sum_{i=1}^{m} \mathbf{w}_{i}^{\alpha k_{0}} = \frac{\mathbf{W}^{\alpha k_{0}} \mathbf{1}_{m}}{m}, \text{ where } \alpha := ak_{0}.$$
 (19)

For simplicity, for each a = 1, 2, 3, ..., define

$$\mathbf{U}^{ak_0} := \left(\mathbf{u}_1^{ak_0}, \cdots, \mathbf{u}_m^{ak_0}\right) = c\mathbf{W}^{ak_0}\mathbf{A}^{ak_0} - \mathbf{\Psi}^{ak_0}, \quad (20)$$

where the last equality holds by the updating step of Algorithm 1: $\mathbf{u}_i^k = \sigma_i m_i^k \overline{\mathbf{w}}_i^k - \nabla f_i(\overline{\mathbf{w}}_i^k)$. And let

$$\mathbf{A}^{i \to a} := \begin{cases} \Pi_{t=(i+1)k_0}^{(a-1)k_0} \mathbf{A}^t, & i = 0, \dots, a-2, \\ \mathbf{I}, & i = a-1, \end{cases}$$

$$\mathbf{d}_i := \frac{\mathbf{1}_m}{m} - \mathbf{e}_i,$$
(21)

where \mathbf{e}_j is the jth column of identity matrix. One can verify that $\phi \mathbf{1}_m^{\top} \mathbf{d}_j = \phi - \phi = 0$. Finally, recall we have defined $c_0 := \left(\frac{80m\sqrt{\ell}}{1-\tau}\right)^2$ and $\tau := \left(1 - \frac{1}{m^{mB}}\right)^{\frac{1}{B}}$, then

$$c \ge c_0 = \left(\frac{80m\sqrt{\ell}}{1-\tau}\right)^2 = \frac{6400m^2\ell}{(1-\tau)^2} \ge \frac{80m\ell}{1-\tau},$$

which gives rise to

$$c^{2}(1-\tau)^{2} - 384m^{2}\ell^{2} \geq \frac{c^{2}(1-\tau)^{2}}{2}, \ c \geq 2\ell,$$

$$\frac{1}{8cm} \geq \frac{800m\ell}{c^{2}(1-\tau)^{2}}, \ \frac{c}{2} \geq \frac{800m^{2}\ell}{3(1-\tau)^{2}}.$$
(22)

B. Key Lemma

Lemma 1. The product of matrix $A^{i\to\alpha}$ is bounded by

$$\left\|\mathbf{A}^{i\to a}\mathbf{d}_{j}\right\|^{2} \le 64m\tau^{2(a-i-1)}, \quad \forall i \le a-1.$$
 (23)

Proof. When i = a - 1, $\mathbf{A}^{i \to a} = \mathbf{I}$ which suffices to

$$\|\mathbf{A}^{i\to a}\mathbf{d}_j\|^2 = \|\mathbf{d}_j\|^2 = \frac{m-1}{m} \le 64m\tau^{2(\alpha-i-1)}.$$
 (24)

When i < a - 1, by Assumption 4, graph G_t^B is connected and thus is strongly connected as it is undirected. Then by [57, Corollary 2], there is a stochastic vector ϕ such that

$$\left| [\mathbf{A}^{i \to a} - \phi \mathbf{1}_m^\top]_{rt} \right| = \left| [\mathbf{A}^{i \to a}]_{rt} - [\phi]_r \right| \le 4\tau^{a - i - 2}, \quad (25)$$

for $\forall r, t \in V$. The above condition leads to

$$\begin{split} \left| \left[(\mathbf{A}^{i \to a} - \boldsymbol{\phi} \mathbf{1}_m^\top) \mathbf{d}_j \right]_r \right| &\leq \max_t \left| \left[\mathbf{A}^{i \to a} - \boldsymbol{\phi} \mathbf{1}_m^\top \right]_{rt} \right| \left\| \mathbf{d}_j \right\|_1 \\ &\leq \frac{8(m-1)\tau^{a-i-2}}{m}, \quad \forall r \in V, \end{split}$$

where $\|\mathbf{w}\|_1$ stands for the 1-norm, and thus

$$\|\mathbf{A}^{i\to a}\mathbf{d}_j\|^2 = \|(\mathbf{A}^{i\to a} - \boldsymbol{\phi}\mathbf{1}_m^\top)\mathbf{d}_j\|^2 \le \frac{64(m-1)^2\tau^{2(a-i-2)}}{m}$$
$$\le 64m\tau^{2(\alpha-i-1)},$$

where the first equality is from $\phi \mathbf{1}_m^{\top} \mathbf{d}_j = 0$, the last inequality is from $m \geq 2$ and

$$\tau^2 = \left(1 - \frac{1}{m^{mB}}\right)^{\frac{2}{B}} \geq \left(1 - \frac{1}{m^{mB}}\right)^2 \geq \left(1 - \frac{1}{m^m}\right)^2 \geq \frac{m-1}{m}.$$

Together with (24), we show the desired result.

Lemma 2. Consider k_0 consecutive iterations: $(a-1)k_0$, $(a-1)k_0 + 1, \ldots, ak_0 - 1$ for some integer a > 0. For $t = 1, \ldots, k_0 - 1$, define

$$\mathbf{Q}^{ak_{0}-k_{0}} := \mathbb{P}_{\Omega} \left(\frac{\mathbf{U}^{(a-1)k_{0}} + \mathbf{\Xi}^{(a-1)k_{0}}}{c} \right) - \frac{\mathbf{U}^{(a-1)k_{0}}}{c},$$

$$\mathbf{Q}^{ak_{0}-t} := \mathbb{P}_{\Omega} \left(\frac{\mathbf{U}^{(a-1)k_{0}} + \mu \mathbf{W}^{ak_{0}-t}}{c+\mu} \right) - \frac{\mathbf{U}^{(a-1)k_{0}} + \mu \mathbf{W}^{ak_{0}-t}}{c+\mu},$$

$$\mathbf{P}^{(a-1)k_{0}} := \sum_{i=0}^{k_{0}-1} \rho^{i} \mathbf{Q}^{ak_{0}-1-i}, \ \rho := \frac{\mu}{c+\mu},$$
(26)

and an error bound

$$e_{\infty} := \sup_{k \ge 1} \left\{ \left\| \mathbb{P}_{\Omega} \left(\mathbf{U}^{k} + \mathbf{\Xi}^{k} \right) - \mathbf{U}^{k} \right\|^{2}, \right.$$
$$\left\| \mathbb{P}_{\Omega} \left(\mathbf{U}^{k} + \mu \mathbf{W}^{k} \right) - \left(\mathbf{U}^{k} + \mu \mathbf{W}^{k} \right) \right\|^{2} \right\}. \tag{27}$$

Then for any $a = 1, 2, 3, \ldots$, it holds that

$$\mathbb{E} \left\| \mathbf{P}^{(a-1)k_0} \right\|^2 \le \frac{k_0 e_{\infty}}{c^2}. \tag{28}$$

Proof. Denote $\mathbf{U}:=\mathbf{U}^{(a-1)k_0}, \mathbf{\Xi}=\mathbf{\Xi}^{(a-1)k_0}, \text{ and } \mathbf{W}:=\mathbf{W}^{ak_0-t}.$ It follows

$$\left\|\mathbf{Q}^{ak_0-k_0}\right\|^2 = \left\|\mathbb{P}_{\Omega}\left(\frac{\mathbf{U}+\mathbf{\Xi}}{c}\right) - \frac{\mathbf{U}}{c}\right\|^2 = \frac{\left\|\mathbb{P}_{\Omega}(\mathbf{U}+\mathbf{\Xi}) - \mathbf{U}\right\|^2}{c^2} \stackrel{(27)}{\leq} \frac{e_{\infty}}{c^2}.$$

As $U^{(a-1)k_0} = U^{ak_0-t}$ for any $t = 1, ..., k_0 - 1$, we have

$$\|\mathbf{Q}^{ak_0-t}\|^2 = \left\| \mathbb{P}_{\Omega} \left(\frac{\mathbf{U} + \mu \mathbf{W}}{c+\mu} \right) - \frac{\mathbf{U} + \mu \mathbf{W}}{c+\mu} \right\|^2$$

$$= \frac{\|\mathbb{P}_{\Omega} (\mathbf{U} + \mu \mathbf{W}) - (\mathbf{U} + \mu \mathbf{W})\|^2}{(c+\mu)^2} \stackrel{(27)}{\leq} \frac{e_{\infty}}{(c+\mu)^2}.$$

Using the above two conditions, we obtain

$$\mathbb{E} \left\| \mathbf{P}^{(a-1)k_0} \right\|^2 = \mathbb{E} \left\| \sum_{i=0}^{k_0 - 1} \rho^i \mathbf{Q}^{ak_0 - 1 - i} \right\|^2 \\
\leq k_0 \sum_{i=0}^{k_0 - 1} \rho^{2i} \mathbb{E} \left\| \mathbf{Q}^{ak_0 - 1 - i} \right\|^2 \\
\leq k_0 \sum_{i=0}^{k_0 - 2} \frac{\rho^{2i} e_{\infty}}{(c + \mu)^2} + \frac{k_0 \rho^{2(k_0 - 1)} e_{\infty}}{c^2} \\
= \frac{k_0 (1 - \rho^{2(k_0 - 1)}) e_{\infty}}{(c + \mu)^2 - \mu^2} + \frac{k_0 \rho^{2(k_0 - 1)} e_{\infty}}{c^2} \leq \frac{k_0 e_{\infty}}{c^2}.$$

The proof is completed.

Hereafter, for notational convenience, let $\alpha := ak_0$.

Lemma 3. Under Assumption 1-2 and setting $c \ge c_0$, it holds,

$$\frac{1}{2cm} \sum_{a=0}^{T-1} \mathbb{E} \left\| \nabla f \left(\boldsymbol{\varpi}^{\alpha} \right) - \boldsymbol{\Psi}^{\alpha} \mathbf{1}_{m} \right\|^{2}
+ \frac{m\ell}{2} \sum_{a=0}^{T-1} \mathbb{E} \left\| \frac{\mathbf{W}^{ak_{0}} (\mathbf{A}^{\alpha} - \mathbb{E} \mathbf{A}^{\alpha}) \mathbf{1}_{m}}{m} \right\|^{2}
\leq \frac{800m\ell}{c^{2}(1-\tau)^{2}} \left(m^{2} \zeta^{2} T + \sum_{a=0}^{T-1} \mathbb{E} \left\| \nabla f \left(\boldsymbol{\varpi}^{\alpha} \right) \right\|^{2}
+ \frac{mc^{2}}{3} \sum_{a=0}^{T-1} \mathbb{E} \left\| \mathbf{P}^{\alpha} \right\|^{2} \right).$$
(29)

Proof. We begin with rewriting the update rule of Algorithm 1 when $\kappa_i = k_0, \forall i$. For $t = 1, 2, \dots, k_0 - 1$

$$\mathbf{W}^{(a-1)k_{0}+1} = \mathbb{P}_{\Omega} \left(\frac{\mathbf{U}^{(a-1)k_{0}} + \mathbf{\Xi}^{(a-1)k_{0}}}{c} \right) \\ \stackrel{(26)}{=} \mathbf{Q}^{(a-1)k_{0}} + \frac{\mathbf{U}^{(a-1)k_{0}}}{c}, \\ \mathbf{W}^{ak_{0}-t+1} = \mathbb{P}_{\Omega} \left(\frac{\mathbf{U}^{(a-1)k_{0}} + \mu \mathbf{W}^{ak_{0}-t}}{c+\mu} \right) \\ \stackrel{(26)}{=} \mathbf{Q}^{ak_{0}-t} + \frac{\mathbf{U}^{(a-1)k_{0}} + \mu \mathbf{W}^{ak_{0}-t}}{c+\mu}.$$
(30)

Using the above condition, we have

$$\begin{split} \mathbf{W}^{ak_0} &\overset{(30)}{=} \mathbf{Q}^{ak_0-1} + \frac{\mathbf{U}^{(a-1)k_0} + \mu \mathbf{W}^{ak_0-1}}{c+\mu} \\ &= \mathbf{Q}^{ak_0-1} + \frac{\mathbf{U}^{(a-1)k_0}}{c+\mu} + \rho \mathbf{W}^{ak_0-1} \\ &\overset{(30)}{=} \mathbf{Q}^{ak_0-1} + \rho \mathbf{Q}^{ak_0-2} + \frac{(1+\rho)\mathbf{U}^{(a-1)k_0}}{c+\mu} + \rho^2 \mathbf{W}^{ak_0-2} \\ &= \cdots \\ &= \sum_{i=0}^{k_0-2} \left(\rho^i \mathbf{Q}^{ak_0-i-1} + \frac{\rho^i \mathbf{U}^{(a-1)k_0}}{c+\mu} \right) + \rho^{k_0-1} \mathbf{W}^{(a-1)k_0+1} \\ &\overset{(30)}{=} \sum_{i=0}^{k_0-2} \rho^i \mathbf{Q}^{ak_0-i-1} + \frac{(1-\rho^{k_0-1})\mathbf{U}^{(a-1)k_0}}{c} + \frac{\rho^{k_0-1}\mathbf{U}^{(a-1)k_0}}{c} \\ &\overset{(26)}{=} \mathbf{P}^{(a-1)k_0} + \frac{\mathbf{U}^{(a-1)k_0}}{c}, \end{split}$$

which further results in

$$\mathbf{W}^{ak_0} = \frac{\mathbf{U}^{(a-1)k_0}}{c} + \mathbf{P}^{(a-1)k_0}$$

$$\stackrel{(20)}{=} \mathbf{W}^{(a-1)k_0} \mathbf{A}^{(a-1)k_0} - \frac{1}{c} \mathbf{\Psi}^{(a-1)k_0} + \mathbf{P}^{(a-1)k_0}$$

$$= \mathbf{W}^{(a-2)k_0} \mathbf{A}^{(a-2)k_0} \mathbf{A}^{(a-1)k_0}$$

$$- \frac{1}{c} \left(\mathbf{\Psi}^{(a-1)k_0} + \mathbf{\Psi}^{(a-2)k_0} \mathbf{A}^{(a-1)k_0} \right)$$

$$+ \left(\mathbf{P}^{(a-1)k_0} + \mathbf{P}^{(a-2)k_0} \mathbf{A}^{(a-1)k_0} \right)$$

$$= \cdots$$

$$= \mathbf{W}^0 \prod_{i=0}^{a-1} \mathbf{A}^{ik_0} - \frac{1}{c} \sum_{i=0}^{a-1} \mathbf{\Psi}^{ik_0} \prod_{q=i+1}^{a-1} \mathbf{A}^{qk_0}$$

$$+ \sum_{i=0}^{a-1} \mathbf{P}^{ik_0} \prod_{q=i+1}^{a-1} \mathbf{A}^{qk_0},$$
(31)

where $\prod_{q=i+1}^{a-1} \mathbf{A}^{qk_0} = \mathbf{I}$ when i = a - 1. With $\mathbf{W}^0 = 0$, we perform two consecutive communication steps and obtain

$$\mathbf{W}^{\alpha} \stackrel{\text{(31,21)}}{=} -\frac{1}{c} \sum_{i=0}^{a-1} \mathbf{\Psi}^{ik_0} \mathbf{A}^{i \to a} + \sum_{i=0}^{a-1} \mathbf{P}^{ik_0} \mathbf{A}^{i \to a}. \tag{32}$$

We divide the proof into four parts:

Part 1. Direct verification enables us to derive the following chain of inequalities,

$$\mathbb{E} \|\nabla f(\boldsymbol{\varpi}^{\alpha}) - \boldsymbol{\Psi}^{\alpha} \mathbf{1}_{m} \|^{2}$$

$$= \mathbb{E} \|\sum_{i=1}^{m} \nabla f_{i} (\boldsymbol{\varpi}^{\alpha}) - \sum_{i=1}^{m} \nabla f_{i} (\overline{\mathbf{w}}_{i}^{\alpha}) \|^{2}$$

$$\leq m \sum_{i=1}^{m} \mathbb{E} \|\nabla f_{i} (\boldsymbol{\varpi}^{\alpha}) - \nabla f_{i} (\overline{\mathbf{w}}_{i}^{\alpha}) \|^{2}$$

$$\leq m\ell^{2} \sum_{i=1}^{m} \mathbb{E} \|\boldsymbol{\varpi}^{\alpha} - \overline{\mathbf{w}}_{i}^{\alpha} \|^{2}$$

$$= m\ell^{2} \sum_{i=1}^{m} \mathbb{E} \|\frac{1}{t_{i}} \sum_{j \in N_{i}^{\alpha}} (\boldsymbol{\varpi}^{\alpha} - \mathbf{w}_{j}^{\alpha}) \|^{2}$$

$$\leq m\ell^{2} \sum_{i=1}^{m} \frac{1}{t_{i}} \sum_{j \in N_{i}^{\alpha}} \mathbb{E} \|\boldsymbol{\varpi}^{\alpha} - \mathbf{w}_{j}^{\alpha} \|^{2},$$

$$(33)$$

where the second equality holds also due to $|N_i^{\alpha}| = m_i^{\alpha} = t_i$ for any i and α .

Part 2. By the global iteration rule, we have

$$\mathbb{E} \left\| \boldsymbol{\varpi}^{\alpha} - \mathbf{w}_{j}^{\alpha} \right\|^{2} \stackrel{(18)}{=} \mathbb{E} \left\| \frac{\mathbf{W}^{\alpha} \mathbf{1}_{m}}{m} - \mathbf{w}_{j}^{\alpha} \right\|^{2} \\
\stackrel{(17)}{=} \mathbb{E} \left\| \frac{\mathbf{W}^{\alpha} \mathbf{1}_{m}}{m} - \mathbf{W}^{\alpha} \mathbf{e}_{j} \right\|^{2} \\
\stackrel{(32)}{=} \mathbb{E} \left\| \left(-\frac{1}{c} \sum_{i=0}^{a-1} \boldsymbol{\Psi}^{ik_{0}} \mathbf{A}^{i \to a} + \sum_{i=0}^{a-1} \mathbf{P}^{ik_{0}} \mathbf{A}^{i \to a} \right) \left(\frac{\mathbf{1}_{m}}{m} - \mathbf{e}_{j} \right) \right\|^{2} \\
\stackrel{(15)}{\leq} \frac{2}{c^{2}} \mathbb{E} \left\| \sum_{i=0}^{a-1} \boldsymbol{\Psi}^{ik_{0}} \mathbf{A}^{i \to a} \mathbf{d}_{j} \right\|^{2} + 2 \mathbb{E} \left\| \sum_{i=0}^{a-1} \mathbf{P}^{ik_{0}} \mathbf{A}^{i \to a} \mathbf{d}_{j} \right\|^{2}.$$

Part 3. Note that the terms in (34) share a similar structure, thus we give a detailed calculation for the first term, and the other one follows the same strategy. First, consider bounding the gradient matrix as follows:

$$\mathbb{E} \left\| \mathbf{\Psi}^{ik_0} \right\|^2 \\
\leq 3\mathbb{E} \left\| \mathbf{\Psi}^{ik_0} - \mathbf{B}^{ik_0} \right\|^2 + 3\mathbb{E} \left\| \nabla f \left(\boldsymbol{\varpi}^{ik_0} \right) \frac{\mathbf{1}_m^{\top}}{m} \right\|^2 \\
+ 3\mathbb{E} \left\| \mathbf{B}^{ik_0} - \nabla f \left(\boldsymbol{\varpi}^{ik_0} \right) \frac{\mathbf{1}_m^{\top}}{m} \right\|^2 \\
\leq 3\ell^2 \sum_{p=1}^m \mathbb{E} \left\| \boldsymbol{\varpi}^{ik_0} - \overline{\mathbf{w}}_p^{ik_0} \right\|^2 + 3m\zeta^2 + \frac{3}{m} \mathbb{E} \left\| \nabla f \left(\boldsymbol{\varpi}^{ik_0} \right) \right\|^2, \tag{35}$$

where $\mathbf{B}^{ik_0} := (\nabla f_1(\boldsymbol{\varpi}^{ik_0}), \cdots, \nabla f_m(\boldsymbol{\varpi}^{ik_0}))$. Moreover, direct calculation derives that

$$\begin{split} & \mathbb{E} \left\| \sum_{i=0}^{a-1} \mathbf{\Psi}^{ik_0} \mathbf{A}^{i \to a} \mathbf{d}_j \right\|^2 \\ &= \sum_{i=0}^{a-1} \mathbb{E} \left\| \mathbf{\Psi}^{ik_0} \mathbf{A}^{i \to a} \mathbf{d}_j \right\|^2 \\ &+ 2 \sum_{i=0}^{a-1} \sum_{t=i+1}^{a-1} \mathbb{E} \left\langle \mathbf{\Psi}^{ik_0} \mathbf{A}^{i \to a} \mathbf{d}_j, \mathbf{\Psi}^{tk_0} \mathbf{A}^{t \to a} \mathbf{d}_j \right\rangle \\ &\leq \sum_{i=0}^{a-1} \mathbb{E} \left\| \mathbf{\Psi}^{ik_0} \right\|^2 \left\| \mathbf{A}^{i \to a} \mathbf{d}_j \right\|^2 \\ &+ 2 \sum_{i=0}^{a-1} \sum_{t=i+1}^{a-1} \mathbb{E} \left\| \mathbf{\Psi}^{ik_0} \right\| \left\| \mathbf{\Psi}^{tk_0} \right\| \left\| \mathbf{A}^{i \to a} \mathbf{d}_j \right\| \left\| \mathbf{A}^{t \to a} \mathbf{d}_j \right\| \\ &\leq \sum_{i=0}^{a-1} \mathbb{E} \left\| \mathbf{\Psi}^{ik_0} \right\|^2 \left\| \mathbf{A}^{i \to a} \mathbf{d}_j \right\|^2 + \sum_{i=0}^{a-1} \sum_{t=i+1}^{a-1} \left(\mathbb{E} \left\| \mathbf{\Psi}^{ik_0} \right\|^2 \right) \\ &+ \mathbb{E} \left\| \mathbf{\Psi}^{tk_0} \right\|^2 \right) \left\| \mathbf{A}^{i \to a} \mathbf{d}_j \right\| \left\| \mathbf{A}^{t \to a} \mathbf{d}_j \right\| \\ &= \sum_{i=0}^{a-1} \mathbb{E} \left\| \mathbf{\Psi}^{ik_0} \right\|^2 \left\| \mathbf{A}^{i \to a} \mathbf{d}_j \right\| \sum_{t=0}^{a-1} \left\| \mathbf{A}^{t \to a} \mathbf{d}_j \right\|, \end{split}$$

which results in

$$\mathbb{E} \left\| \sum_{i=0}^{a-1} \mathbf{\Psi}^{ik_0} \mathbf{A}^{i \to a} \mathbf{d}_j \right\|^2$$

$$\leq \sum_{i=0}^{a-1} \mathbb{E} \left\| \mathbf{\Psi}^{ik_0} \right\|^2 64m\tau^{\alpha-i-1} \sum_{t=0}^{a-1} \tau^{a-t-1}$$

$$\leq \sum_{i=0}^{a-1} \mathbb{E} \left\| \mathbf{\Psi}^{ik_0} \right\|^2 \frac{64m\tau^{a-i-1}}{1-\tau}.$$
(36)

Similar reasoning to show the above condition enables us to prove that

$$\mathbb{E} \left\| \sum_{i=0}^{a-1} \mathbf{P}^{ik_0} \mathbf{A}^{i \to a} \mathbf{d}_j \right\|^2 \leq \sum_{i=0}^{a-1} \mathbb{E} \left\| \mathbf{P}^{ik_0} \right\|^2 \frac{64m\tau^{a-i-1}}{1-\tau}.$$

Part 4. The above two conditions immediately give rise to

$$\begin{split} &\sum_{a=0}^{T-1} \sum_{q=1}^{m} \mathbb{E} \left\| \boldsymbol{\varpi}^{\alpha} - \overline{\mathbf{w}}_{q}^{\alpha} \right\|^{2} \\ &\stackrel{(15)}{\leq} \sum_{a=0}^{T-1} \sum_{q=1}^{m} \frac{1}{t_{q}} \sum_{j \in \mathcal{N}_{q}^{\alpha}} \mathbb{E} \left\| \boldsymbol{\varpi}^{\alpha} - \mathbf{w}_{j}^{\alpha} \right\|^{2} \\ &\stackrel{(34)}{\leq} \sum_{a=0}^{T-1} \sum_{q=1}^{m} \frac{1}{t_{q}} \sum_{j \in \mathcal{N}_{q}^{\alpha}} \left(\frac{2}{c^{2}} \mathbb{E} \left\| \sum_{i=0}^{a-1} \boldsymbol{\Psi}^{ik_{0}} \mathbf{A}^{i \to a} \mathbf{d}_{j} \right\|^{2} \right) \\ &+ 2 \mathbb{E} \left\| \sum_{i=0}^{a-1} \mathbf{P}^{ik_{0}} \mathbf{A}^{i \to a} \mathbf{d}_{j} \right\|^{2} \right) \\ &\leq \sum_{a=0}^{T-1} \sum_{q=1}^{m} \frac{1}{t_{q}} \sum_{j \in \mathcal{N}_{q}^{\alpha}} \sum_{i=0}^{a-1} \left(\frac{1}{c^{2}} \mathbb{E} \left\| \boldsymbol{\Psi}^{ik_{0}} \right\|^{2} \right) \\ &+ \mathbb{E} \left\| \mathbf{P}^{ik_{0}} \right\|^{2} \right) \frac{128m\tau^{a-i-1}}{1-\tau} \\ &= \sum_{a=0}^{T-1} m \sum_{i=0}^{a-1} \left(\frac{1}{c^{2}} \mathbb{E} \left\| \boldsymbol{\Psi}^{ik_{0}} \right\|^{2} + \mathbb{E} \left\| \mathbf{P}^{ik_{0}} \right\|^{2} \right) \frac{128m\tau^{a-i-1}}{1-\tau} \\ &\leq \frac{128m^{2}}{(1-\tau)^{2}} \sum_{i=0}^{T-1} \left(\frac{1}{c^{2}} \mathbb{E} \left\| \boldsymbol{\Psi}^{ik_{0}} \right\|^{2} + \mathbb{E} \left\| \mathbf{P}^{ik_{0}} \right\|^{2} \right) \\ &\stackrel{(35)}{\leq} \frac{128m^{2}}{c^{2}(1-\tau)^{2}} \sum_{i=0}^{T-1} \left(3\ell^{2} \sum_{p=1}^{m} \mathbb{E} \left\| \boldsymbol{\varpi}^{ik_{0}} - \overline{\mathbf{w}}_{p}^{ik_{0}} \right\|^{2} + 3m\zeta^{2} \\ &+ \frac{3}{m} \mathbb{E} \left\| \nabla f \left(\boldsymbol{\varpi}^{ik_{0}} \right) \right\|^{2} \right) + \frac{128m^{2}}{(1-\tau)^{2}} \sum_{i=0}^{T-1} \mathbb{E} \left\| \mathbf{P}^{ik_{0}} \right\|^{2}, \end{aligned}$$
which further leads to

$$384m^{3}\zeta^{2}T + 384m \sum_{a=0}^{T-1} \mathbb{E} \|\nabla f(\boldsymbol{\varpi}^{\alpha})\|^{2}$$

$$+ 128m^{2}c^{2} \sum_{a=0}^{T-1} \mathbb{E} \|\mathbf{P}^{\alpha}\|^{2}$$

$$\geq \left(c^{2}(1-\tau)^{2} - 384m^{2}\ell^{2}\right) \sum_{a=0}^{T-1} \sum_{q=1}^{m} \mathbb{E} \|\boldsymbol{\varpi}^{\alpha} - \overline{\mathbf{w}}_{q}^{\alpha}\|^{2}$$

$$\stackrel{(22)}{\geq} \frac{c^{2}(1-\tau)^{2}}{2} \sum_{a=0}^{T-1} \sum_{q=1}^{m} \mathbb{E} \|\boldsymbol{\varpi}^{\alpha} - \overline{\mathbf{w}}_{q}^{\alpha}\|^{2}.$$

This results in

$$\sum_{\alpha=0}^{T-1} \sum_{p=1}^{m} \mathbb{E} \left\| \boldsymbol{\varpi}^{\alpha} - \overline{\mathbf{w}}_{p}^{\alpha} \right\|^{2}$$

$$\leq \frac{800m}{c^{2}(1-\tau)^{2}} \left(m^{2} \zeta^{2} T + \sum_{a=0}^{T-1} \mathbb{E} \left\| \nabla f \left(\boldsymbol{\varpi}^{\alpha} \right) \right\|^{2} + \frac{mc^{2}}{3} \sum_{a=0}^{T-1} \mathbb{E} \left\| \mathbf{P}^{\alpha} \right\|^{2} \right).$$
(37)

Finally, we note $\mathbb{E}\mathbf{A}^{\alpha}$ is a doubly stochastic matrix. Consequently, $\frac{\mathbf{W}^{\alpha}\mathbb{E}\mathbf{A}^{\alpha}\mathbf{1}_{m}}{m} = \frac{\mathbf{W}^{\alpha}\mathbf{1}_{m}}{m} = \boldsymbol{\varpi}^{\alpha}$, which results in

$$\frac{m\ell}{2} \mathbb{E} \left\| \frac{\mathbf{W}^{\alpha} (\mathbf{A}^{\alpha} - \mathbb{E} \mathbf{A}^{\alpha}) \mathbf{1}_{m}}{m} \right\|^{2} = \frac{m\ell}{2} \mathbb{E} \left\| \frac{\mathbf{W}^{\alpha} \mathbf{A}^{\alpha} \mathbf{1}_{m}}{m} - \frac{\mathbf{W}^{\alpha} \mathbf{1}_{m}}{m} \right\| \\
= \frac{m\ell}{2} \mathbb{E} \left\| \frac{1}{m} \sum_{p=1}^{m} \left(\boldsymbol{\varpi}^{\alpha} - \overline{\mathbf{w}}_{p}^{\alpha} \right) \right\|^{2} \\
\leq \frac{\ell}{2} \sum_{p=1}^{m} \mathbb{E} \left\| \boldsymbol{\varpi}^{\alpha} - \overline{\mathbf{w}}_{p}^{\alpha} \right\|^{2}.$$
(38)

Combining (37), we obtain

$$\frac{1}{2cm} \sum_{a=0}^{T-1} \mathbb{E} \left\| \nabla f \left(\boldsymbol{\varpi}^{\alpha} \right) - \boldsymbol{\Psi}^{\alpha} \mathbf{1}_{m} \right\|^{2} \\
+ \frac{m\ell}{2} \sum_{a=0}^{T-1} \mathbb{E} \left\| \frac{\mathbf{W}^{\alpha} (\mathbf{A}^{\alpha} - \mathbb{E} \mathbf{A}^{\alpha}) \mathbf{1}_{m}}{m} \right\|^{2} \\
\leq \left(\frac{\ell^{2}}{2c} + \frac{\ell}{2} \right) \sum_{a=0}^{T-1} \sum_{p=1}^{m} \mathbb{E} \left\| \boldsymbol{\varpi}^{\alpha} - \overline{\mathbf{w}}_{p}^{\alpha} \right\|^{2} \\
\leq \ell \sum_{a=0}^{T-1} \sum_{p=1}^{m} \mathbb{E} \left\| \boldsymbol{\varpi}^{\alpha} - \overline{\mathbf{w}}_{p}^{\alpha} \right\|^{2} \\
\leq \frac{800m\ell}{c^{2}(1-\tau)^{2}} (m^{2}\zeta^{2}T + \sum_{a=0}^{T-1} \mathbb{E} \left\| \nabla f \left(\boldsymbol{\varpi}^{\alpha} \right) \right\|^{2} \\
+ \frac{mc^{2}}{3} \sum_{a=0}^{T-1} \mathbb{E} \left\| \mathbf{P}^{\alpha} \right\|^{2}).$$

The whole proof is finished.

Lemma 4. Under Assumption 1 and setting $c \ge c_0$, it holds

$$\frac{1}{4cm} \mathbb{E} \left\| \nabla f \left(\boldsymbol{\varpi}^{\alpha} \right) \right\|^{2} \\
\leq \mathbb{E} f \left(\boldsymbol{\varpi}^{\alpha} \right) - \mathbb{E} f \left(\boldsymbol{\varpi}^{\alpha+1} \right) + \frac{3c}{2} \mathbb{E} \left\| \mathbf{P}^{\alpha} \right\|^{2} \\
+ \frac{1}{2cm} \mathbb{E} \left\| \nabla f \left(\boldsymbol{\varpi}^{\alpha} \right) - \boldsymbol{\Psi}^{\alpha} \mathbf{1}_{m} \right\|^{2} + \frac{m\ell}{2} \left\| \frac{\mathbf{W}^{\alpha} \triangle \mathbf{A}^{\alpha} \mathbf{1}_{m}}{m} \right\|^{2}.$$
(39)

Proof. Firstly, we have

$$\mathbb{E}\left\langle \nabla f\left(\boldsymbol{\varpi}^{\alpha} - \frac{\boldsymbol{\Psi}^{\alpha} \mathbf{1}_{m}}{cm}\right), \frac{\mathbf{P}^{\alpha} \mathbf{1}_{m}}{m} \right\rangle \\
\leq \frac{5cm}{4} \mathbb{E} \left\| \frac{\mathbf{P}^{\alpha} \mathbf{1}_{m}}{m} \right\|^{2} + \frac{1}{5cm} \mathbb{E} \left\| \nabla f\left(\boldsymbol{\varpi}^{\alpha} - \frac{\boldsymbol{\Psi}^{\alpha} \mathbf{1}_{m}}{cm}\right) \right\|^{2} \\
\leq \frac{5cm}{4} \mathbb{E} \left\| \frac{\mathbf{P}^{\alpha} \mathbf{1}_{m}}{m} \right\|^{2} + \frac{1}{4cm} \mathbb{E} \left\| \nabla f\left(\boldsymbol{\varpi}^{\alpha}\right) \right\|^{2} \\
+ \frac{1}{cm} \mathbb{E} \left\| \nabla f\left(\boldsymbol{\varpi}^{\alpha} - \frac{\boldsymbol{\Psi}^{\alpha} \mathbf{1}_{m}}{cm}\right) - \nabla f\left(\boldsymbol{\varpi}^{\alpha}\right) \right\|^{2} \\
\leq \frac{5cm}{4} \mathbb{E} \left\| \frac{\mathbf{P}^{\alpha} \mathbf{1}_{m}}{m} \right\|^{2} + \frac{1}{4cm} \mathbb{E} \left\| \nabla f\left(\boldsymbol{\varpi}^{\alpha}\right) \right\|^{2} \\
+ \frac{1}{c} \sum_{i=1}^{m} \mathbb{E} \left\| \nabla f_{i}\left(\boldsymbol{\varpi}^{\alpha} - \frac{\boldsymbol{\Psi}^{\alpha} \mathbf{1}_{m}}{cm}\right) - \nabla f_{i}\left(\boldsymbol{\varpi}^{\alpha}\right) \right\|^{2} \\
\leq \frac{5cm}{4} \mathbb{E} \left\| \frac{\mathbf{P}^{\alpha} \mathbf{1}_{m}}{m} \right\|^{2} + \frac{\ell^{2}}{c^{3}m} \mathbb{E} \left\| \boldsymbol{\Psi}^{\alpha} \mathbf{1}_{m} \right\|^{2} + \frac{1}{4cm} \mathbb{E} \left\| \nabla f\left(\boldsymbol{\varpi}^{\alpha}\right) \right\|^{2}.$$

Then the Lipschitz continuity enables the following conditions,

$$\mathbb{E}f(\boldsymbol{\varpi}^{\alpha} - \frac{\boldsymbol{\Psi}^{\alpha} \mathbf{1}_{m}}{cm}) \\
\leq \mathbb{E}f(\boldsymbol{\varpi}^{\alpha}) - \frac{1}{cm} \mathbb{E} \left\langle \nabla f(\boldsymbol{\varpi}^{\alpha}), \boldsymbol{\Psi}^{\alpha} \mathbf{1}_{m} \right\rangle + \frac{m\ell}{2} \mathbb{E} \left\| \frac{\boldsymbol{\Psi}^{\alpha} \mathbf{1}_{m}}{cm} \right\|^{2} \\
= \mathbb{E}f(\boldsymbol{\varpi}^{\alpha}) + \frac{m\ell}{2} \mathbb{E} \left\| \frac{\boldsymbol{\Psi}^{\alpha} \mathbf{1}_{m}}{cm} \right\|^{2} + \frac{1}{2cm} \mathbb{E} \left\| \nabla f(\boldsymbol{\varpi}^{\alpha}) - \boldsymbol{\Psi}^{\alpha} \mathbf{1}_{m} \right\|^{2} \\
- \frac{1}{2cm} \mathbb{E} \left\| \nabla f(\boldsymbol{\varpi}^{\alpha}) \right\|^{2} - \frac{1}{2cm} \mathbb{E} \left\| \boldsymbol{\Psi}^{\alpha} \mathbf{1}_{m} \right\|^{2} \\
= \mathbb{E}f(\boldsymbol{\varpi}^{\alpha}) + \frac{\ell - c}{2c^{2}m} \mathbb{E} \left\| \boldsymbol{\Psi}^{\alpha} \mathbf{1}_{m} \right\|^{2} - \frac{1}{2cm} \mathbb{E} \left\| \nabla f(\boldsymbol{\varpi}^{\alpha}) \right\|^{2} \\
+ \frac{1}{2cm} \mathbb{E} \left\| \nabla f(\boldsymbol{\varpi}^{\alpha}) - \boldsymbol{\Psi}^{\alpha} \mathbf{1}_{m} \right\|^{2}. \tag{41}$$

In addition, one can check that

$$\frac{\ell^2}{c^3 m} + \frac{\ell - c}{2c^2 m} \stackrel{(22)}{\le} \frac{1}{2c^2 m} \left(\frac{2\ell^2}{2\ell} + \ell - 2\ell\right) = 0,$$

$$\frac{5mc + 2m\ell}{4} \stackrel{(22)}{\le} \frac{5mc + mc}{4} \le \frac{3mc}{2}.$$
(42)

Moreover, by observing that $\frac{1}{m}\mathbf{W}^{\alpha}\mathbb{E}\mathbf{A}^{\alpha}\mathbf{1}_{m} = \frac{1}{m}\mathbf{W}^{\alpha}\mathbf{1}_{m} = \boldsymbol{\varpi}^{\alpha}$ and $\triangle \mathbf{A}^{\alpha} := \mathbf{A}^{\alpha} - \mathbb{E}\mathbf{A}^{\alpha}$, it follows

$$\begin{split} \boldsymbol{\varpi}^{\alpha+1} &\stackrel{(19)}{=} \frac{\mathbf{W}^{\alpha+1}\mathbf{1}_m}{m} \stackrel{(31)}{=} \frac{\mathbf{W}^{\alpha}\mathbf{A}^{\alpha}\mathbf{1}_m}{m} - \frac{\boldsymbol{\Psi}^{\alpha}\mathbf{1}_m}{cm} + \frac{\mathbf{P}^{\alpha}\mathbf{1}_m}{m} \\ &= \frac{\mathbf{W}^{\alpha}\mathbb{E}\mathbf{A}^{\alpha}\mathbf{1}_m}{m} - \frac{\boldsymbol{\Psi}^{\alpha}\mathbf{1}_m}{cm} + \frac{\mathbf{P}^{\alpha}\mathbf{1}_m}{m} + \frac{\mathbf{W}^{\alpha}\triangle\mathbf{A}^{\alpha}\mathbf{1}_m}{m} \\ &= \boldsymbol{\varpi}^{\alpha} - \frac{\boldsymbol{\Psi}^{\alpha}\mathbf{1}_m}{cm} + \frac{\mathbf{P}^{\alpha}\mathbf{1}_m}{m} + \frac{\mathbf{W}^{\alpha}\triangle\mathbf{A}^{\alpha}\mathbf{1}_m}{m}, \end{split}$$

which by $\boldsymbol{\nu}^{\alpha}:=\boldsymbol{\varpi}^{\alpha}-\frac{\boldsymbol{\Psi}^{\alpha}\mathbf{1}_{m}}{cm}+\frac{\mathbf{P}^{\alpha}\mathbf{1}_{m}}{m}$ and $\mathbb{E}\triangle\mathbf{A}^{\alpha}=0$ yields

$$\mathbb{E}f\left(\boldsymbol{\varpi}^{\alpha+1}\right) \\
\stackrel{(14)}{\leq} \mathbb{E}f\left(\boldsymbol{\nu}^{\alpha}\right) + \mathbb{E}\langle\nabla f\left(\boldsymbol{\nu}^{\alpha}\right), \frac{\mathbf{W}^{\alpha}\triangle\mathbf{A}^{\alpha}\mathbf{1}_{m}}{m}\rangle + \frac{m\ell}{2} \left\| \frac{\mathbf{W}^{\alpha}\triangle\mathbf{A}^{\alpha}\mathbf{1}_{m}}{m} \right\|^{2} \\
&= \mathbb{E}f\left(\boldsymbol{\nu}^{\alpha}\right) + \frac{m\ell}{2} \left\| \frac{\mathbf{W}^{\alpha}\triangle\mathbf{A}^{\alpha}\mathbf{1}_{m}}{m} \right\|^{2} \\
\stackrel{(14)}{\leq} \mathbb{E}f\left(\boldsymbol{\varpi}^{\alpha} - \frac{\boldsymbol{\Psi}^{\alpha}\mathbf{1}_{m}}{cm}\right) + \mathbb{E}\left\langle\nabla f\left(\boldsymbol{\varpi}^{\alpha} - \frac{\boldsymbol{\Psi}^{\alpha}\mathbf{1}_{m}}{cm}\right), \frac{\mathbf{P}^{\alpha}\mathbf{1}_{m}}{m}\right\rangle \\
&+ \frac{m\ell}{2} \left\| \frac{\mathbf{W}^{\alpha}\triangle\mathbf{A}^{\alpha}\mathbf{1}_{m}}{m} \right\|^{2} + \frac{m\ell}{2} \mathbb{E} \left\| \frac{\mathbf{P}^{\alpha}\mathbf{1}_{m}}{m} \right\|^{2} \\
&\leq \mathbb{E}f\left(\boldsymbol{\varpi}^{\alpha}\right) + \frac{\ell-c}{2c^{2}m} \mathbb{E} \left\|\boldsymbol{\Psi}^{\alpha}\mathbf{1}_{m}\right\|^{2} - \frac{1}{2cm} \mathbb{E} \left\|\nabla f\left(\boldsymbol{\varpi}^{\alpha}\right)\right\|^{2} \\
&+ \frac{1}{2cm} \mathbb{E} \left\|\nabla f\left(\boldsymbol{\varpi}^{\alpha}\right) - \boldsymbol{\Psi}^{\alpha}\mathbf{1}_{m}\right\|^{2} + \frac{m\ell}{2} \mathbb{E} \left\| \frac{\mathbf{P}^{\alpha}\mathbf{1}_{m}}{m} \right\|^{2} \\
&+ \mathbb{E}\left\langle\nabla f\left(\boldsymbol{\varpi}^{\alpha} - \frac{\boldsymbol{\Psi}^{\alpha}\mathbf{1}_{m}}{cm}\right), \frac{\mathbf{P}^{\alpha}\mathbf{1}_{m}}{m}\right\rangle + \frac{m\ell}{2} \left\| \frac{\mathbf{W}^{\alpha}\triangle\mathbf{A}^{\alpha}\mathbf{1}_{m}}{m} \right\|^{2} \\
&\leq \mathbb{E}f\left(\boldsymbol{\varpi}^{\alpha}\right) + \left(\frac{\ell^{2}}{c^{3}m} + \frac{\ell-c}{2c^{2}m}\right) \mathbb{E} \left\|\boldsymbol{\Psi}^{\alpha}\mathbf{1}_{m}\right\|^{2} \\
&- \frac{1}{4cm} \mathbb{E} \left\|\nabla f\left(\boldsymbol{\varpi}^{\alpha}\right)\right\|^{2} + \frac{1}{2cm} \mathbb{E} \left\|\nabla f\left(\boldsymbol{\varpi}^{\alpha}\right) - \boldsymbol{\Psi}^{\alpha}\mathbf{1}_{m}\right\|^{2} \\
&+ \frac{5mc+2m\ell}{4} \mathbb{E} \left\| \frac{\mathbf{P}^{\alpha}\mathbf{1}_{m}}{m} \right\|^{2} + \frac{m\ell}{2} \left\| \frac{\mathbf{W}^{\alpha}\triangle\mathbf{A}^{\alpha}\mathbf{1}_{m}}{m} \right\|^{2} \\
&\leq \mathbb{E}f\left(\boldsymbol{\varpi}^{\alpha}\right) - \frac{1}{4cm} \mathbb{E} \left\|\nabla f\left(\boldsymbol{\varpi}^{\alpha}\right)\right\|^{2} + \frac{3c}{2} \mathbb{E} \left\|\mathbf{P}^{\alpha}\right\|^{2} \\
&+ \frac{1}{2cm} \mathbb{E} \left\|\nabla f\left(\boldsymbol{\varpi}^{\alpha}\right) - \boldsymbol{\Psi}^{\alpha}\mathbf{1}_{m}\right\|^{2} + \frac{m\ell}{2} \left\| \frac{\mathbf{W}^{\alpha}\triangle\mathbf{A}^{\alpha}\mathbf{1}_{m}}{m} \right\|^{2},
\end{cases}$$

finishing the proof.

C. Proof of Theorem 1

Proof. Summing (39) from $\alpha = 0$ to $\alpha = T - 1$ gives

$$\frac{1}{4cm} \sum_{a=0}^{T-1} \mathbb{E} \left\| \nabla f \left(\boldsymbol{\varpi}^{\alpha} \right) \right\|^{2} \\
\leq \sum_{a=0}^{T-1} \left(\mathbb{E} f \left(\boldsymbol{\varpi}^{\alpha} \right) - \mathbb{E} f \left(\boldsymbol{\varpi}^{\alpha+1} \right) + \frac{3c}{2} \mathbb{E} \left\| \mathbf{P}^{\alpha} \right\|^{2} \\
+ \frac{1}{2cm} \mathbb{E} \left\| \nabla f \left(\boldsymbol{\varpi}^{\alpha} \right) - \boldsymbol{\Psi}^{\alpha} \mathbf{1}_{m} \right\|^{2} + \frac{m\ell}{2} \left\| \frac{\mathbf{W}^{\alpha} \triangle \mathbf{A}^{\alpha} \mathbf{1}_{m}}{m} \right\|^{2} \right) \\
= \mathbb{E} f \left(\boldsymbol{\varpi}^{0} \right) - \mathbb{E} f \left(\boldsymbol{\varpi}^{T} \right) + \sum_{a=0}^{T-1} \left(\frac{3c}{2} \mathbb{E} \left\| \mathbf{P}^{\alpha} \right\|^{2} \right) \\
+ \frac{1}{2cm} \mathbb{E} \left\| \nabla f \left(\boldsymbol{\varpi}^{\alpha} \right) - \boldsymbol{\Psi}^{\alpha} \mathbf{1}_{m} \right\|^{2} + \frac{m\ell}{2} \left\| \frac{\mathbf{W}^{\alpha} \triangle \mathbf{A}^{\alpha} \mathbf{1}_{m}}{m} \right\|^{2} \right) \\
\leq f \left(0 \right) - f^{*} + \frac{3c}{2} \sum_{a=0}^{T-1} \mathbb{E} \left\| \mathbf{P}^{\alpha} \right\|^{2} + \frac{800m\ell}{c^{2}(1-\tau)^{2}} \left(m^{2} \zeta^{2} T \right) \\
+ \sum_{a=0}^{T-1} \mathbb{E} \left\| \nabla f \left(\boldsymbol{\varpi}^{\alpha} \right) \right\|^{2} + \frac{mc^{2}}{3} \sum_{a=0}^{T-1} \mathbb{E} \left\| \mathbf{P}^{\alpha} \right\|^{2} \\
\leq f \left(0 \right) - f^{*} + 2c \sum_{a=0}^{T-1} \mathbb{E} \left\| \mathbf{P}^{\alpha} \right\|^{2} \\
+ \frac{c_{0} m^{2} \zeta^{2} T}{8mc^{2}} + \frac{1}{8cm} \sum_{a=0}^{T-1} \mathbb{E} \left\| \nabla f \left(\boldsymbol{\varpi}^{\alpha} \right) \right\|^{2},$$

which immediately delivers that

$$\frac{1}{8cm} \sum_{a=0}^{T-1} \mathbb{E} \|\nabla f(\boldsymbol{\varpi}^{\alpha})\|^{2} \\
\leq f(0) - f^{*} + \frac{c_{0}m^{2}\zeta^{2}T}{8mc^{2}} + 2c \sum_{a=0}^{T-1} \mathbb{E} \|\mathbf{P}^{\alpha}\|^{2} \\
\leq f(0) - f^{*} + \frac{c_{0}m^{2}\zeta^{2}T}{8mc^{2}} + \frac{2k_{0}e_{\infty}}{c}.$$

This condition suffices to

$$\begin{split} & \frac{1}{T} \sum_{a=0}^{T-1} \mathbb{E} \left\| \nabla f \left(\boldsymbol{\varpi}^{\alpha} \right) \right\|^{2} \\ & \leq \frac{8cm(f(0) - f^{*})}{T} + \frac{c_{0}m^{2}\zeta^{2} + 16mck_{0}e_{\infty}}{c}, \end{split}$$

as desired.

D. Proof of Theorem 2

Proof. At each iteration k, node i accesses its raw dataset only during the gradient computation $\nabla f_i(\overline{\mathbf{w}}_i^k)$, i.e., at steps ak_0 . By Assumption 5, the sensitivity of this computation is u_i . According to the Gaussian mechanism [?, Theorem 3.22], adding Gaussian noise with variance ϱ_i ensures that the gradient computation satisfies (ε, δ) -differential privacy. Now let $\mathcal{A}^k(D)$ be the operations of each iteration k of Algorithm 1. Then it can be decomposed as a series of parallel operations $\{\mathcal{A}_i^k(D_i): i \in V\}$ on all nodes, namely, $\mathcal{A}^k(D) = (\mathcal{A}_1^k(D_1), \mathcal{A}_2^k(D_2), \cdots, \mathcal{A}_m^k(D_m))$. By the parallel composition theorem [?], the overall privacy budget is not affected by nodes' number m because each data point is accessed only once across the local operations. As a result, each iteration $\mathcal{A}^k(D)$ is also (ε, δ) -differential private.

E. Proof of Theorem 3

Proof. During ak_0 iterations, the noises are added when only on steps $k=0,k_0,\ldots,(a-1)k_0$. Therefore, the algorithm with ak_0 steps can be considered as an adaptive composition of $(\mathcal{A}_0(D),\mathcal{A}_1(D),\cdots,\mathcal{A}_{a-1}(D))$, which by [?, Theorem 3.2] enables the conclusion.